

# Vacuum Stress and Closed Paths in Rectangles, Pistons, and Pistols

S. A. Fulling<sup>a,b,\*</sup>, L. Kaplan<sup>c</sup>, K. Kirsten<sup>d</sup>, Z. H. Liu<sup>b</sup>,  
K. A. Milton<sup>e</sup>

<sup>a</sup>*Department of Mathematics, Texas A&M University, College Station, TX,  
77843-3368 USA*

<sup>b</sup>*Department of Physics, Texas A&M University, College Station, TX,  
77843-4242 USA*

<sup>c</sup>*Department of Physics, Tulane University, New Orleans, LA, 70118 USA*

<sup>d</sup>*Department of Mathematics, Baylor University, Waco, TX, 76798-7328 USA*

<sup>e</sup>*H. L. Dodge Department of Physics and Astronomy, University of Oklahoma,  
Norman, OK, 73019-2061 USA*

---

## Abstract

Rectangular cavities are solvable models that nevertheless touch on many of the controversial or mysterious aspects of the vacuum energy of quantum fields. This paper is a thorough study of the two-dimensional scalar field in a rectangle by the method of images, or closed classical (or optical) paths, which is exact in this case. For each point  $\mathbf{r}$  and each specularly reflecting path beginning and ending at  $\mathbf{r}$ , we provide formulas for all components of the stress tensor  $T_{\mu\nu}(\mathbf{r})$ , for all values of the curvature coupling constant  $\xi$  and all values of an ultraviolet cutoff parameter. Arbitrary combinations of Dirichlet and Neumann conditions on the four sides can be treated. The total energy is also investigated, path by path. These results are used in an attempt to clarify the physical reality of the repulsive (outward) force on the sides of the box predicted by calculations that neglect both boundary divergences and the exterior of the box. Previous authors have studied “piston” geometries that avoid these problems and have found the force to be attractive. We consider a “pistol” geometry that comes closer to the original problem of a box with a movable lid. We find again an attractive force, although its origin and detailed behavior are somewhat different from the piston case. However, the pistol (and the piston) model can be criticized for extending idealized boundary conditions into short distances where they are physically implausible. Therefore, it is of interest to see whether leaving the ultraviolet cutoff finite yields results that are more plausible. We then find that the force depends strongly on a geometrical parameter; it can be made repulsive, but only by forcing that parameter into the regime where the model is least convincing physically.

*Key words:* Casimir, vacuum energy, parallelepiped, ultraviolet cutoff

## 1 Introduction

### 1.1 History and motivation

Rectangular cavities are perhaps the most frequently studied geometries in connection with vacuum (Casimir) energy. Nevertheless, there are still worthwhile things to say about them. Although exactly solvable, they exhibit many features that are subjects of current research and debate in the broader context of quantum vacuum energy: boundary divergences, corner effects, sometimes surprising signs, and sometimes revealing connections with geometry through the spectrum of periodic and other closed classical paths (or optical rays).

A complete listing of previous literature is impossible, but we summarize what we see as the most important historical developments.

Lukosz [1] calculated the interior vacuum energy of the electromagnetic field in a (3D) perfectly conducting parallelepiped, using zeta-function regularization, and predicted a repulsive (outward) force for many aspect ratios, including the cube. Ambjørn and Wolfram [2] extended such calculations to a wide variety of dimensions, fields, and boundary conditions. Actor [3] emphasized that divergences in the total energy must be understood in terms of the local behavior of the field near boundaries and boundary singularities (edges and corners), and calculated the local zeta function for the 3D scalar field. For earlier, closely related discussions of a rectangular waveguide and various other systems, see [4,5]. All these works were done in the framework of zeta functions [6,7,8], but in practice, in the special case of rectangular cavities, functional equations for Epstein zeta functions are used to convert zeta-regularized sums over eigenvalues into what are, in effect, zeta-regularized sums over classical paths. (In [9] a transition to an ultraviolet cutoff was also made at this step.)

The calculation of vacuum energy via classical paths (also called optical rays) [10,11,12,13,14,15,16,17] leads naturally to more physical regularizations associated with separation of points in the Green functions of the theory. For rectangular parallelepipeds such calculations are exact (no stationary-phase approximations are required) and reduce to the classic method of images. Although they did not discuss vacuum energy, Balian and Bloch [18] used the

---

\* Corresponding author.

*Email address:* `fulling@math.tamu.edu` (S. A. Fulling).

3D parallelepiped as a principal example in their landmark study of the relation between periodic orbits and oscillations in the eigenvalue density, and their catalog of periodic and other closed orbits is the best starting point for a study of the rectangle. Hacyan et al. [19] calculated the full stress tensor for the electromagnetic field in a box by a Green-function approach; along the way, they showed how to reduce the electromagnetic problem to scalar fields with mixed Dirichlet and Neumann boundary conditions via Hertz potentials. In this connection see also [20]. (Contrary to the impression left by some papers on the global problem, a local investigation of electromagnetism cannot be split into pure Dirichlet and pure Neumann problems, even when a decomposition into TE and TM modes exists.)

At this point we should mention the work of Ford and Svaiter [21], which showed that physically motivated cutoffs could convert divergences into finite effects clearly localized near boundaries. This theme has been repeatedly visited since then [22,23,15,24,25,26] and will play a major role in the present work.

Cavalcanti [27] rejuvenated the field by introducing the piston model (for a 2D scalar field), discussed in detail in Sec. 4 and illustrated in Fig 6. (Similar ideas were advanced earlier by Svaiter et al. [28].) The motivation for the piston is that the calculation of the force on the piston plate is unaffected by either uncompensated divergences or unknown forces from the exterior. The conclusion of [27] is that the force is always attractive (inward). That paper used both zeta and cutoff regularization, but still starting from the eigenvalue spectrum. Hertzberg et al. [29,30] extended the piston model to dimension 3 and to the electromagnetic field, and they analyzed it in terms of closed paths (but without the close attention to locally defined quantities that we provide here). From that point of view, the repulsive nature of the Lukosz force is attributable to a particular type of path moving parallel to the plate and producing an energy proportional to the piston displacement. (It is essentially the Casimir energy associated with the walls perpendicular to the movable plate.) But such energy is also present in the exterior part of the piston shaft, and therefore these paths make no net contribution to the force. What is left of the Lukosz force is attractive. This effect shows up even more clearly in the two-dimensional model (Sec. 4).

Rodriguez et al. [31,32] have made a numerical study of two conducting rectangular objects in a narrow passage, a model closely akin to the pistons and pistons we discuss here. They conclude that the distance to the confining walls influences the attraction between the blocks, and their analysis makes use of the local stress tensor. In [33] that model is approached by the method of closed optical paths.

Illuminating though the piston has been, it does not settle the original issue

of the physical reality of the force calculated by Lukosz [1] and others. The existence of a Casimir-like energy in the exterior part of the piston shaft says nothing about what happens when that part of the shaft is removed, the plate remaining free to move (see Fig. 7 in Sec. 5). The “finite part” of that force is robust, in the sense that all reasonable prescriptions for calculating it give the same answer. It can be obtained by differentiating the total energy, or by integrating the pressure over the movable boundary. It can be obtained by zeta-function regularization or by ultraviolet cutoffs, and within the latter framework the choice of cutoff function dictates the relative sizes of the cutoff-dependent terms but not the structure of the series nor the numerical value of the finite term [27, Appendix B]. Is the object of this consensus a meaningless number? One of our goals is to investigate to what extent it has physical significance.

The opinion expressed in [29] is that “Without [the piston shaft] (or some open region that allows rigid motion of the partition) the Casimir energy of the parallelepiped is, in fact, cutoff dependent. If the cutoff dependence is somehow ignored, a repulsive force . . . remains as an artifact.” We agree that a correct calculation of the force on the piston must include the effect of the piston shaft, and that the net effect is attractive. We do not agree that the repulsive force associated with the interior can be dismissed as an artifact of naively discarding a divergent term. The scenario indicated in Fig. 7, a box with a movable lid, is a well-defined problem of relative motion of rigid bodies, just as much as the piston is; cutoff-dependent energies associated with the rigid boundaries cannot affect the force. The difficulties of analyzing Fig. 7 are, first, that the effects of the corners and gaps in that geometry are hard to calculate (see, however, [34,35,36,37,38] and, on a different tack, [39,40]), and, second, that the idealized Casimir theory is not physically applicable to very small separations of the bodies. We evade the first problem by considering another scenario, the “pistol” (Fig. 8), which should still exhibit the uncompensated Lukosz force on a flat boundary. However, we find that the situation is then confounded by a strong countervailing attractive force associated with the Casimir energy in the narrow gap surrounding the “bullet”. Moreover, one now runs up against the second problem, which cannot be treated seriously within the limits of our methodology. A crude model of a “real” boundary can be easily obtained, however, by maintaining a finite cutoff of atomic dimensions. The result is that the force depends sensitively on how tightly the “bullet” fits into the “barrel”. If the fit is loose, the Lukosz force is overwhelmed by the corresponding force associated with the gap surrounding the bullet, and the net force is attractive. If the fit is tight, the gap force can be made repulsive or even fine-tuned to vanish, as originally hoped; unfortunately, that is the regime in which one is least justified in taking the model seriously. All we claim is that external forces opposing the Lukosz force are model-dependent and might, in principle, be controlled so as to demonstrate the existence of the Lukosz force.

In this paper we consider strictly the two-dimensional scalar field, usually with Dirichlet boundary conditions, although we sometimes lapse into the three-dimensional electromagnetic terminology (such as “conductor”) for conceptual discussions. It is intended that three-dimensional generalizations will be presented elsewhere [41]. Sec. 2 presents a thorough analysis, by means of classical paths, of all components of the stress (energy-momentum) tensor in a rectangle. Sec. 3 does the same for the energy and also the pressure and force on one side. Contributions are recorded for each path (or class of similar paths) separately, with comments on their physical or geometrical significance to the extent that we can discern it. The results are stated for all values of the curvature, or conformal, coupling constant,  $\xi$  (see (2) and (4)), and all values of the parameter in an exponential ultraviolet cutoff. For the most part, they are stated for any combination of Dirichlet and Neumann conditions on the four sides of the box. A brief account of this part of the work was published previously [42], along with evidence that the gravitational effects of boundaries in the “renormalized” theory without cutoff can be understood (and believed) as the distributional limit of the predictions of the cutoff theory, thereby providing a true renormalization. In the rest of the paper we restrict to the Dirichlet condition. The piston is reviewed from our point of view in Sec. 4. Sec. 5 introduces the pistol model and treats it in the Dirichlet theory. Sec. 6 investigates the pistol with a finite cutoff.

*A remark on terminology:* Many authors, including some of ourselves on previous occasions (e.g., [23]), use the term “renormalized energy” to refer to the finite part of a regularized energy when the latter is expanded as a series in the cutoff parameter. Strictly speaking, “renormalization” refers to the process of obtaining physically observable probability amplitudes by absorbing suitable divergent and finite contributions into redefinitions of physical parameters (couplings, masses, etc.) appearing in the bare Lagrangian. Ideally, all renormalizations in the first sense should either be associated with renormalizations in the second sense or be justified by cancellations of divergent terms coming from different sources. Yet in the absence of a completed theory, one must often talk about renormalization in the first sense without having an obvious counterterm or cancellation, and there seems to be no convenient substitute terminology. Much of our work in this paper has to do, in fact, with exhibiting cancellations, and [42] and its planned sequels have to do with gravitational counterterms. When we use “renormalization” or “renormalized” in the first sense, we have always either put the word in quotation marks or accompanied it by the word “naive”, depending on context.

## 1.2 Basic formalism

We are concerned here with the massless scalar wave equation

$$\frac{\partial^2 \phi}{\partial (x^0)^2} = \nabla^2 \phi \quad (1)$$

in a cavity  $\Omega$  together with a Dirichlet ( $\phi = 0$ ) or Neumann ( $\hat{\mathbf{n}} \cdot \nabla \phi = 0$ ) condition on each part of the boundary of  $\Omega$ . We write  $H$  for the corresponding positive self-adjoint operator:  $H = -\nabla^2$  with boundary conditions understood. The eigenvalues of  $H$  are positive, with the possible exception (in the totally Neumann case) of a constant eigenfunction with eigenvalue zero. The formulas in this subsection are presented for arbitrary spatial dimension  $d$ , but in the next section we specialize to  $d = 2$ .

The field equation (1) is obtained canonically from the curved-space action and Lagrangian

$$S = \int_{\Omega} L \sqrt{|g|} d^{d+1}x, \quad L = \frac{1}{2} [g^{\mu\nu} \partial_{\mu} \phi \partial_{\nu} \phi + \xi R \phi^2], \quad (2)$$

by taking the variation with respect to  $\phi$  and then setting the metric to its flat-space value,  $g_{\mu\nu} = \eta_{\mu\nu}$ . (Our tensorial sign conventions are that  $\eta_{00} < 0$ , but  $T_{00} > 0$  for normal matter.) The stress tensor is defined by

$$T^{\mu\nu} = \frac{2}{\sqrt{|g|}} \frac{\delta S}{\delta g_{\mu\nu}}. \quad (3)$$

It reduces in flat space-time (after use of the equation of motion, (1)) to

$$T_{\mu\nu} = (1 - 2\xi) \partial_{\mu} \phi \partial_{\nu} \phi + (2\xi - \frac{1}{2}) \eta_{\mu\nu} \partial_{\lambda} \phi \partial^{\lambda} \phi - 2\xi \phi \partial_{\mu} \partial_{\nu} \phi. \quad (4)$$

In (2)  $R$  is the curvature scalar, and  $\xi$  labels different possible gravitational couplings. In curved space different values of  $\xi$  are different theories; after the reduction to flat space the field equation is independent of  $\xi$ , but the stress tensors are different. It turns out [see (7)] that changing  $\xi$  changes  $T_{00}$  only by a divergence, and therefore the total energy  $E = \int_{\Omega} T_{00} d\mathbf{r}$  is independent of  $\xi$ , at least classically, under Dirichlet or Neumann boundary conditions. (A Robin boundary condition [43,23,44],  $\hat{\mathbf{n}} \cdot \nabla \phi = \gamma \phi$ , would require a boundary term to be added to the action (2). There results a  $\xi$ -dependent boundary term in  $E$ , which vanishes when  $\xi = \frac{1}{4}$ . Similar remarks apply to models with delta function potentials [24,25,26].) There are three natural choices of  $\xi$ :

$\xi = 0$ : minimal coupling, which simplifies the Lagrangian and curved-space field equation;

$\xi = \xi_d$ : conformal coupling,

$$\xi_d \equiv \frac{d-1}{4d}; \quad \xi_2 = \frac{1}{8}, \quad \xi_3 = \frac{1}{6}, \quad \xi_\infty = \frac{1}{4}, \quad (5)$$

which results in the mildest behavior of the quantized field near the boundary;

$\xi = \frac{1}{4}$ : the coupling that eliminates the Robin boundary energy, which also simplifies the relation between the stress tensor and the total energy, as we shall see.

It is convenient to adopt  $\xi = \frac{1}{4}$  as the base value and to define  $\beta = \xi - \frac{1}{4}$  to parametrize the coupling. Thus we write

$$T_{\mu\nu}(\xi) \equiv T_{\mu\nu}(\frac{1}{4}) + \Delta T_{\mu\nu} \quad (6)$$

and obtain

$$T_{00}(\frac{1}{4}) = \frac{1}{2} \left[ \left( \frac{\partial\phi}{\partial x^0} \right)^2 - \phi \nabla^2 \phi \right], \quad \Delta T_{00} = -2\beta \nabla \cdot (\phi \nabla \phi), \quad (7)$$

$$T_{0j}(\frac{1}{4}) = \frac{1}{2} \left[ \frac{\partial\phi}{\partial x^0} \frac{\partial\phi}{\partial x_j} - \phi \frac{\partial^2\phi}{\partial x^0 \partial x_j} \right], \quad \Delta T_{0j} = -2\beta \frac{\partial}{\partial x^0} \left( \phi \frac{\partial\phi}{\partial x_j} \right), \quad (8)$$

$$T_{jk}(\frac{1}{4}) = \frac{1}{2} \left[ \frac{\partial\phi}{\partial x_j} \frac{\partial\phi}{\partial x_k} - \phi \frac{\partial^2\phi}{\partial x_j \partial x_k} \right],$$

$$\Delta T_{jk} = -2\beta \left[ \frac{\partial\phi}{\partial x_j} \frac{\partial\phi}{\partial x_k} + \phi \frac{\partial^2\phi}{\partial x_j \partial x_k} \right] \quad \text{when } j \neq k, \quad (9)$$

$$T_{jj}(\frac{1}{4}) = \frac{1}{2} \left[ \left( \frac{\partial\phi}{\partial x_j} \right)^2 - \phi \frac{\partial^2\phi}{\partial x_j^2} \right],$$

$$\Delta T_{jj} = -2\beta \left[ \left( \frac{\partial\phi}{\partial x^0} \right)^2 - \sum_{k \neq j} \left( \frac{\partial\phi}{\partial x_k} \right)^2 + \phi \frac{\partial^2\phi}{\partial x_j^2} \right]. \quad (10)$$

The trace of the tensor is

$$T_\lambda^\lambda = - \left( \frac{1}{2} + 2\beta d \right) \left[ \left( \frac{\partial\phi}{\partial x^0} \right)^2 - (\nabla\phi)^2 \right], \quad (11)$$

which vanishes for the conformal coupling,  $\beta = -(4d)^{-1}$ .

When the theory is canonically quantized, the vacuum expectation value of the stress tensor is expressed formally in terms of the normal modes

$$\varphi_n = \frac{1}{\sqrt{2\omega_n}} \phi_n(\mathbf{r}) e^{-i\omega_n x^0}, \quad H\phi_n = \omega_n^2 \phi_n, \quad \|\phi_n\| = 1,$$

as

$$\langle T_{\mu\nu}(\mathbf{r}) \rangle = \sum_{n=1}^{\infty} T_{\mu\nu}[\varphi_n, \varphi_n^*]. \quad (12)$$

(The Neumann zero mode, when it exists, is omitted and ignored. If included and treated properly, it would add a continuous energy spectrum [45, Appendix].) The notation in (12) means that in each of the bilinear terms in (7)–(10), the field  $\phi$  is replaced by a mode function in one factor and by its complex conjugate in the other. (When the factors are not the same, the product should be symmetrized.) In particular,

$$\langle T_{00}(\tfrac{1}{4}) \rangle = \frac{1}{2} \sum_n \omega_n |\phi_n(\mathbf{r})|^2. \quad (13)$$

Integrating  $T_{00}(\tfrac{1}{4})$  over  $\Omega$  gives the expected formal sum for the total energy,

$$\langle E \rangle = \frac{1}{2} \sum_n \omega_n. \quad (14)$$

As promised earlier, we regularize all these divergent sums with an exponential ultraviolet cutoff. It is convenient to start from the (Poisson) cylinder kernel,

$$T(t, \mathbf{r}, \mathbf{r}') \equiv \sum_{n=1}^{\infty} \phi_n(\mathbf{r}) \phi_n(\mathbf{r}')^* e^{-t\omega_n} = \langle \mathbf{r} | e^{-t\sqrt{H}} | \mathbf{r}' \rangle. \quad (15)$$

(Here  $t$  is not the physical time.) Then

$$\langle T_{00}(\tfrac{1}{4}) \rangle_t = -\frac{1}{2} \frac{\partial T}{\partial t}(t, \mathbf{r}, \mathbf{r}), \quad (16)$$

$$\langle E \rangle_t = -\frac{1}{2} \frac{\partial}{\partial t} T(t), \quad T(t) \equiv \int_{\Omega} T(t, \mathbf{r}, \mathbf{r}) d\mathbf{r}. \quad (17)$$



To obtain  $\langle \Delta T_{00} \rangle$  and the other components of  $\langle T_{\mu\nu} \rangle$  one needs a more primitive cylinder kernel,

$$\bar{T}(t, \mathbf{r}, \mathbf{r}') = - \sum_{n=1}^{\infty} \frac{1}{\omega_n} \phi_n(\mathbf{r}) \phi_n(\mathbf{r}')^* e^{-t\omega_n}. \quad (18)$$

Then  $T = \frac{\partial \bar{T}}{\partial t}$  and

$$\langle \Delta T_{00} \rangle_t = \beta \nabla_{\mathbf{r}} \cdot [\nabla_{\mathbf{r}'} \bar{T}(t, \mathbf{r}, \mathbf{r}')]_{\mathbf{r}'=\mathbf{r}}. \quad (19)$$

In terms of partial differential equations,  $T$  and  $\bar{T}$  are characterized by the elliptic equation

$$\frac{\partial^2 T}{\partial t^2} = -\nabla^2 T \quad (20)$$

along with the imposed spatial boundary conditions, the initial condition

$$T(0, \mathbf{r}, \mathbf{r}') = \delta(\mathbf{r} - \mathbf{r}') = \frac{\partial \bar{T}}{\partial t}(0, \mathbf{r}, \mathbf{r}'),$$

and the requirement of boundedness as  $t \rightarrow +\infty$ . (The Green function  $\bar{T}$  can be introduced differently, either as twice the Euclidean Green function in  $\mathbf{R} \times \Omega$  with its source on  $t = 0$ , or through an analytic continuation to imaginary time of the Wightman or Feynman two-point function.)

The vacuum expectation values of the summands in (8) are identically zero, as expected from the mode-by-mode time-reversal invariance. For the other components one obtains

$$\langle T_{jj}(\frac{1}{4}) \rangle_t = \frac{1}{8} \left[ -2 \frac{\partial^2}{\partial x_j \partial x'_j} + \frac{\partial^2}{\partial x_j^2} + \frac{\partial^2}{\partial x'_j{}^2} \right] \bar{T}, \quad (21)$$

$$\langle \Delta T_{jj} \rangle_t = \frac{\beta}{2} \left[ 2 \frac{\partial^2}{\partial t^2} - 2 \sum_{k \neq j} \frac{\partial^2}{\partial x_k \partial x'_k} + \frac{\partial^2}{\partial x_j^2} + \frac{\partial^2}{\partial x'_j{}^2} \right] \bar{T}, \quad (22)$$

$$\langle T_{jk}(\frac{1}{4}) \rangle_t = \frac{1}{8} \left[ \frac{\partial^2}{\partial x_j \partial x_k} + \frac{\partial^2}{\partial x'_j \partial x'_k} - \frac{\partial^2}{\partial x_j \partial x'_k} - \frac{\partial^2}{\partial x'_j \partial x_k} \right] \bar{T}, \quad (23)$$

$$\langle \Delta T_{jk} \rangle_t = \frac{\beta}{2} \left[ \frac{\partial^2}{\partial x_j \partial x_k} + \frac{\partial^2}{\partial x'_j \partial x'_k} + \frac{\partial^2}{\partial x_j \partial x'_k} + \frac{\partial^2}{\partial x'_j \partial x_k} \right] \bar{T}, \quad (24)$$

where it is understood that  $\mathbf{r}'$  is to be set equal to  $\mathbf{r}$  at the final step.

## 2 The stress tensor

### 2.1 Preliminaries

We now restrict attention to dimension 2 and write  $x$  for  $x_1$  and  $y$  for  $x_2$ . Define

$$A \equiv \frac{\partial T}{\partial t} = \frac{\partial^2 \bar{T}}{\partial t^2}, \quad (25)$$

$$B_1 \equiv \frac{1}{2} \left( \frac{\partial^2 \bar{T}}{\partial x^2} + \frac{\partial^2 \bar{T}}{\partial x'^2} \right), \quad B_2 \equiv \frac{1}{2} \left( \frac{\partial^2 \bar{T}}{\partial y^2} + \frac{\partial^2 \bar{T}}{\partial y'^2} \right), \quad (26)$$

$$C_1 \equiv \frac{\partial^2 \bar{T}}{\partial x \partial x'}, \quad C_2 \equiv \frac{\partial^2 \bar{T}}{\partial y \partial y'}, \quad (27)$$

$$D_{12} \equiv \frac{1}{2} \left( \frac{\partial^2 \bar{T}}{\partial x \partial y'} + \frac{\partial^2 \bar{T}}{\partial y \partial x'} \right), \quad (28)$$

$$E_{12} \equiv \frac{1}{2} \left( \frac{\partial^2 \bar{T}}{\partial x \partial y} + \frac{\partial^2 \bar{T}}{\partial x' \partial y'} \right). \quad (29)$$

(The subscripts on  $D$  and  $E$  are merely to facilitate later generalization to higher dimensions.) Then from (16), (19), and (21)–(24) we have

$$\langle T_{00}(\frac{1}{4}) \rangle_t = -\frac{1}{2} A, \quad (30)$$

$$\langle \Delta T_{00} \rangle_t = \beta(B_1 + B_2 + C_1 + C_2), \quad (31)$$

$$\langle T_{01}(\frac{1}{4}) \rangle_t = 0 = \langle \Delta T_{01} \rangle_t, \quad \text{etc.}, \quad (32)$$

$$\langle T_{11}(\frac{1}{4}) \rangle_t = \frac{1}{4}(B_1 - C_1), \quad \text{etc.}, \quad (33)$$

$$\langle \Delta T_{11} \rangle_t = \beta(A + B_1 - C_2), \quad \text{etc.}, \quad (34)$$

$$\langle T_{12}(\frac{1}{4}) \rangle_t = \frac{1}{4}(-D_{12} + E_{12}), \quad (35)$$

$$\langle \Delta T_{12} \rangle_t = \beta(D_{12} + E_{12}). \quad (36)$$

In (30)–(36) it is understood that  $\mathbf{r}' = \mathbf{r}$ .

### 2.2 Path classes and energy density

The cylinder kernels in infinite two-dimensional space are

$$\bar{T}(t, \mathbf{r}, \mathbf{r}') = -\frac{1}{2\pi} (t^2 + |\mathbf{r} - \mathbf{r}'|^2)^{-1/2}, \quad (37)$$

$$T(t, \mathbf{r}, \mathbf{r}') = \frac{t}{2\pi} (t^2 + |\mathbf{r} - \mathbf{r}'|^2)^{-3/2}. \quad (38)$$

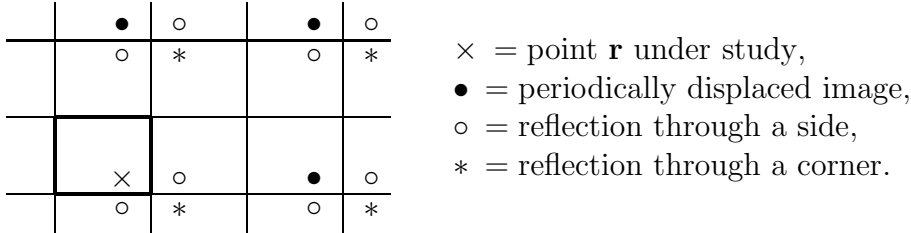


Fig. 1. A point in a rectangle and its images relevant to Dirichlet and Neumann boundary conditions (cf. [18, Sec. 9.A]). Image points fall into three classes according to whether the number of reflections is *even* in both dimensions, one, or neither. The first case corresponds to periodic displacements. Points of the third class are joined to  $\mathbf{r}$  by lines that pass through an intersection point of the lattice of extended rectangle sides — i.e., an image of a corner of the rectangle.

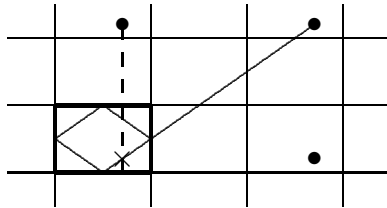


Fig. 2. Two periodic paths (one solid, one dashed) are shown, both within the rectangle and in the covering space.

Because of its central importance, we shall discuss the energy density,  $\langle T_{00}(\frac{1}{4}) \rangle$ , along with the construction of the cylinder kernel for the rectangle, path by path. For rectangular parallelepipeds of any dimension, with any combination of Dirichlet, Neumann, and periodic boundary conditions, the construction of any kernel (Green function) as a sum over classical paths reduces to the classic “method of images” (and yields the exact answer). For a rectangle the array of image points appears in Fig. 1. To every path is associated a sign,  $(-1)^\eta$ , where  $\eta$  is the number of Dirichlet sides struck by the path. (If a path hits a corner, both sides are counted, and the path reflects back upon itself.) The image sum for  $\bar{T}$  is not absolutely convergent, but the derivatives of the series, from which observable quantities are calculated, are convergent.

Following Cavalcanti [27] we take the rectangle to have horizontal and vertical dimensions  $a$  and  $b$ , horizontal and vertical coordinates  $x$  and  $y$ , and horizontal image-displacement indices  $j$  and  $k$ . (We occasionally still find it necessary to use  $j$  and  $k$  as tensor indices, but never in the same equation as the image indices.) Thus the contribution of a typical periodic path (see Fig. 2) to  $\bar{T}$  is

$$\bar{T}_{Pjk} = -\frac{(-1)^\eta}{2\pi} [t^2 + (2ja + x' - x)^2 + (2kb + y' - y)^2]^{-1/2}. \quad (39)$$

From (30) and (25) we obtain

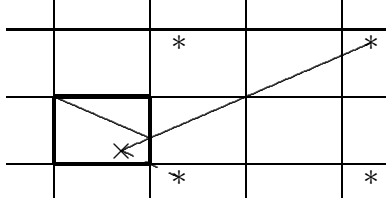


Fig. 3. Two corner paths. Inside the rectangle such paths bounce back from a corner and retrace themselves. The shortest such paths have lengths arbitrarily close to 0.

$$\begin{aligned} \langle T_{00}(\frac{1}{4}) \rangle_{tPjk} &= -\frac{(-1)^\eta}{4\pi} \left[ t^2 + (2ja)^2 + (2kb)^2 \right]^{-5/2} \\ &\quad \times \left[ -2t^2 + (2ja)^2 + (2kb)^2 \right], \end{aligned} \quad (40)$$

which is independent of  $\mathbf{r}$ . Also, one finds from (31) and (26)–(27) that  $C_j = -B_j$  in this case and hence

$$\langle \Delta T_{00} \rangle_{tPjk} = 0. \quad (41)$$

These two results are expected and related: Since  $\Delta T_{00}$  is a total divergence and hence must integrate to 0, and since the energy from a periodic path is independent of position in the rectangle,  $\langle \Delta T_{00} \rangle_{tPjk}$  must be identically zero. Finally, note that if the boundaries are all Dirichlet or all Neumann,  $\eta$  is even and hence  $\langle T_{00} \rangle_{0Pjk}$  is always negative.

Next, consider the simple and interesting case of a corner path:

$$\bar{T}_{Cjk} = -\frac{(-1)^\eta}{2\pi} \left[ t^2 + (2ja - x' - x)^2 + (2kb - y' - y)^2 \right]^{-1/2}. \quad (42)$$

This time one finds that  $C_j = +B_j$  and  $B_1 + B_2 = -A$ , so that

$$\begin{aligned} \langle T_{00}(\frac{1}{4}) \rangle_{tCjk} &= \frac{1}{4\beta} \langle \Delta T_{00} \rangle_{tCjk} \\ &= -\frac{(-1)^\eta}{4\pi} \left[ t^2 + (2ja - 2x)^2 + (2kb - 2y)^2 \right]^{-5/2} \\ &\quad \times \left[ -2t^2 + (2ja - 2x)^2 + (2kb - 2y)^2 \right]. \end{aligned} \quad (43)$$

That is, the two terms in  $\langle T_{00} \rangle_{tCjk}$  are proportional, and, in particular,  $\langle T_{00} \rangle_{tCjk}$  vanishes for minimal coupling ( $\beta = -\frac{1}{4}$ ). These seeming coincidences are probably related to the fact that the integral of  $\langle T_{00} \rangle_{tCjk}$  over the rectangle must vanish (see Sec. 3). Note that the quantity is a function of the distance to  $\mathbf{r}$  from the corner or corner-image concerned (see Fig. 3). Again it is negative as  $t \rightarrow 0$  whenever all the boundary conditions are of the same type.

The situation is slightly more complicated for paths that “bounce” in one dimension while being periodic (or fixed) in the other. The number of reflections

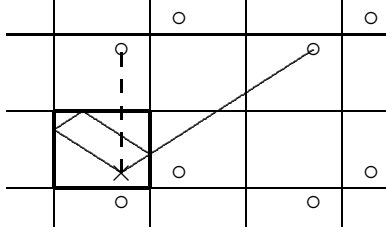


Fig. 4. Two side paths of the vertical subclass. The dashed path is a direct perpendicular reflection (retracing itself), with length approaching 0 as  $\mathbf{r}$  approaches the top boundary. The solid path combines a reflection from the top with a periodic horizontal drift; its length is bounded away from 0.

is now odd, and the energy density turns out to be positive for Dirichlet conditions and negative for Neumann, at least for  $\beta$  near 0. We call these paths “vertical side paths” if the bounce is off a horizontal side (see Fig. 4); this includes, in particular, the strictly vertical paths ( $j = 0$ ). In those cases we have

$$\overline{T}_{Vjk} = -\frac{(-1)^\eta}{2\pi} \left[ t^2 + (2ja + x' - x)^2 + (2kb - y' - y)^2 \right]^{-1/2}, \quad (44)$$

$$\begin{aligned} \langle T_{00}(\tfrac{1}{4}) \rangle_{tVjk} &= -\frac{(-1)^\eta}{4\pi} \left[ t^2 + (2ja)^2 + (2kb - 2y)^2 \right]^{-5/2} \\ &\quad \times \left[ -2t^2 + (2ja)^2 + (2kb - 2y)^2 \right], \end{aligned} \quad (45)$$

$$\begin{aligned} \langle \Delta T_{00} \rangle_{tVjk} &= \frac{\beta(-1)^\eta}{\pi} \left[ t^2 + (2ja)^2 + (2kb - 2y)^2 \right]^{-5/2} \\ &\quad \times \left[ t^2 + (2ja)^2 - 2(2kb - 2y)^2 \right]. \end{aligned} \quad (46)$$

These quantities depend only on  $y$ , not  $x$ ; in other words, such a term is a function of the distance from a wall or an image of a wall. In this case the two terms in the energy density are distinctly different, so it pays to write out the total explicitly:

$$\begin{aligned} \langle T_{00} \rangle_{tVjk} &= \frac{(-1)^\eta}{\pi} \left[ t^2 + (2ja)^2 + (2kb - 2y)^2 \right]^{-5/2} \\ &\quad \times \left[ \left( \beta + \frac{1}{2} \right) t^2 + \left( \beta - \frac{1}{4} \right) (2ja)^2 - \left( 2\beta + \frac{1}{4} \right) (2kb - 2y)^2 \right]. \end{aligned} \quad (47)$$

The most interesting observation here is that the coefficient of  $(2kb - 2y)^2$  vanishes for conformal coupling ( $\beta = -\frac{1}{8}$ ). When  $j = 0$  and  $k = 0$  or  $1$ , the energy density for  $t = 0$  generically has  $O(y^{-3})$  divergences at the boundary, but those divergences are removed in the conformal case; this is as close as one

comes in a rectangle to the well known fact that the energy density between infinite parallel plates is *constant* in the case of conformal coupling.

Formulas for horizontal side paths are easily obtained from (44)–(47) by interchanging the roles of the two dimensions.

### 2.3 The other components

From (33)–(36) and (39), (42), (44), one finds the spatial components (pressure and shear stress). We omit the formula for the 22 component when it is obvious from the 11 formula.

*Periodic paths:*

$$\begin{aligned} \langle T_{11}(\tfrac{1}{4}) \rangle_{tPjk} &= \frac{(-1)^\eta}{4\pi} \left[ t^2 + (2ja)^2 + (2kb)^2 \right]^{-5/2} \\ &\quad \times \left[ t^2 - 2(2ja)^2 + (2kb)^2 \right], \end{aligned} \quad (48)$$

$$\langle T_{12}(\tfrac{1}{4}) \rangle_{tPjk} = -\frac{3(-1)^\eta}{\pi} \left[ t^2 + (2ja)^2 + (2kb)^2 \right]^{-5/2} jkb, \quad (49)$$

$$\langle \Delta T_{11} \rangle_{tPjk} = 0 = \langle \Delta T_{12} \rangle_{tPjk}. \quad (50)$$

Thus the stress tensor associated with a periodic path does not depend upon the conformal parameter, nor upon the coordinates. The individual terms  $\langle T_{12} \rangle$  are nonzero, but they add to zero when summed over either  $j$  or  $k$ , as reflection symmetry requires.

*Corner paths:*

$$\langle T_{11}(\tfrac{1}{4}) \rangle_{tCjk} = \langle T_{12}(\tfrac{1}{4}) \rangle_{tCjk} = 0, \quad (51)$$

$$\begin{aligned} \langle \Delta T_{11} \rangle_{tCjk} &= -\frac{\beta(-1)^\eta}{\pi} \left[ t^2 + (2ja - 2x)^2 + (2kb - 2y)^2 \right]^{-5/2} \\ &\quad \times \left[ t^2 + (2ja - 2x)^2 - 2(2kb - 2y)^2 \right], \end{aligned} \quad (52)$$

$$\begin{aligned} \langle \Delta T_{12} \rangle_{tCjk} &= -\frac{12\beta(-1)^\eta}{\pi} \left[ t^2 + (2ja - 2x)^2 + (2kb - 2y)^2 \right]^{-5/2} \\ &\quad \times (ja - x)(kb - y). \end{aligned} \quad (53)$$

In addition to (and in contrast to) the remarks about the energy density made below (43), we observe: (1) The spatial components of the corner-path stress tensor vanish when  $\xi = \frac{1}{4}$  (whereas the energy density vanishes when  $\xi = 0$ ). So far we have no intuitive explanation of this fact. (2) The spatial components are no longer functions of corner-image distances alone, though they do have (for  $t = 0$ ) an  $O(|\mathbf{r}|^{-3})$  dependence on corner-image coordinates, as the energy density does. (3) When  $\beta \neq 0$  there is a nonzero  $\langle T_{12} \rangle$ , which does not vanish even when summed. However, if we evaluate it on a boundary (such as  $x = (\text{integer}) \times a$ ), where it would have a clear physical interpretation as a shear force on the wall of the box, then it does vanish when summed.

*Vertical paths:*

$$\begin{aligned} \langle T_{11}(\tfrac{1}{4}) \rangle_{tVjk} &= \frac{(-1)^\eta}{4\pi} \left[ t^2 + (2ja)^2 + (2kb - 2y)^2 \right]^{-5/2} \\ &\quad \times \left[ t^2 - 2(2ja)^2 + (2kb - 2y)^2 \right], \end{aligned} \quad (54)$$

$$\begin{aligned} \langle \Delta T_{11} \rangle_{tVjk} &= -\frac{\beta(-1)^\eta}{\pi} \left[ t^2 + (2ja)^2 + (2kb - 2y)^2 \right]^{-5/2} \\ &\quad \times \left[ t^2 + (2ja)^2 - 2(2kb - 2y)^2 \right], \end{aligned} \quad (55)$$

$$\langle T_{22} \rangle_{tVjk} = 0 = \langle T_{12} \rangle_{tVjk} = 0. \quad (56)$$

In addition to the remarks surrounding (44)–(47), observe that  $\langle T_{\nu 2} \rangle = 0$  for all  $\nu$ . That is understandable: there is otherwise no way to satisfy the conservation laws (60) for  $\mu = 1$  and  $\mu = 2$  by functions that depend only on  $y$  but are not constant.

*Horizontal paths:*

$$\langle T_{11} \rangle_{tHjk} = 0 = \langle T_{12} \rangle_{tHjk} = 0, \quad (57)$$

$$\begin{aligned} \langle T_{22}(\tfrac{1}{4}) \rangle_{tHjk} &= \frac{(-1)^\eta}{4\pi} \left[ t^2 + (2ja - 2x)^2 + (2kb)^2 \right]^{-5/2} \\ &\quad \times \left[ t^2 + (2ja - 2x)^2 - 2(2kb)^2 \right], \end{aligned} \quad (58)$$

$$\begin{aligned} \langle \Delta T_{22} \rangle_{tHjk} &= -\frac{\beta(-1)^\eta}{\pi} \left[ t^2 + (2ja - 2x)^2 + (2kb)^2 \right]^{-5/2} \\ &\quad \times \left[ t^2 - 2(2ja - 2x)^2 + (2kb)^2 \right]. \end{aligned} \quad (59)$$

Observe that  $\langle T_{12} \rangle = 0$  for *all* side paths.

For the formulas above one can verify the conservation law

$$-\frac{\partial}{\partial x^0} \langle T_{0\mu} \rangle + \frac{\partial}{\partial x_1} \langle T_{1\mu} \rangle + \frac{\partial}{\partial x_2} \langle T_{2\mu} \rangle = 0 \quad (\mu = 0, 1, 2). \quad (60)$$

Here the first term is always 0, because the quantities do not depend upon time (not to be confused with the regularization parameter  $t$ ). In the conformal case,  $\beta = -\frac{1}{8}$ , one also has tracelessness,

$$-\langle T_{00} \rangle + \langle T_{11} \rangle + \langle T_{22} \rangle = 0. \quad (61)$$

These identities hold for all  $t$ , not just  $t = 0$ .

### 3 Energy and force

#### 3.1 Introductory remarks

In this section the results of the previous one will be used to calculate the contribution of each image term to the total energy,  $E$ , of the scalar field in the rectangle, and consequently the force,  $-\frac{\partial E}{\partial a}$ , on the rectangle's right side. We are concerned here only with the force from inside the rectangle; "piston" arrangements in which it is possible to calculate or estimate forces from outside will be considered in later sections. Consequently, uncompensated divergent terms arise as the cutoff parameter  $t$  is taken to 0, and such terms need to be identified and systematically isolated for later physical scrutiny.

The sign of Casimir energies and forces has long been a topic of great interest and mystery, and one of the motivations of our research has been to see what light the decomposition into image terms, for which the sign is easy to understand, can shed on such questions. The following discussion is easy to present for arbitrary spatial dimension  $d$ .

The cylinder kernel in  $\mathbf{R}^d$  is

$$T(t, \mathbf{r}, \mathbf{r}') = C(d) t(t^2 + |\mathbf{r} - \mathbf{r}'|^2)^{-(d+1)/2}, \quad C(d) \equiv \frac{\Gamma(\frac{d+1}{2})}{\pi^{\frac{d+1}{2}}}. \quad (62)$$

Consequently, in the  $d$ -dimensional analogues of the constructions in Sec. 2.2



all the terms in the energy density  $\langle T_{00}(\frac{1}{4}) \rangle$  will have the form

$$-\frac{(-1)^n}{2} \frac{\partial}{\partial t} [t(t^2 + W)^{-s}] = (-1)^n \frac{(s - \frac{1}{2})t^2 - \frac{1}{2}W}{(t^2 + W)^{s+1}}, \quad (63)$$

where  $W$  is some nonnegative function of  $\mathbf{r}$ . If  $W > 0$ , the limit as  $t \rightarrow 0$  is  $-\frac{1}{2}(-1)^n W^{-s}$ ; for pure Neumann boundary conditions it is always negative, while for pure Dirichlet conditions it will be positive whenever the number of nonperiodic (bounce) dimensions is odd for the path concerned. If  $W = 0$ , the small- $t$  behavior is  $(-1)^n (s - \frac{1}{2})t^{-2s}$ , divergent and opposite in sign to the other terms.

Now we consider integrating over a coordinate  $u$  when  $W = V + (mL - u)^2$  with  $V \geq 0$ :

$$I \equiv \int_0^L \frac{(s - \frac{1}{2})t^2 - \frac{1}{2}[V + (mL - u)^2]}{[t^2 + V + (mL - u)^2]^{s+1}} du.$$

By the mean value theorem for integrals,

$$I = L \frac{(s - \frac{1}{2})t^2 - \frac{1}{2}[V + (mL - \zeta)^2]}{[t^2 + V + (mL - \zeta)^2]^{s+1}},$$

where  $0 < \zeta < L$  and  $\zeta$  may depend on  $t$ . But for us  $s$  is always greater than or equal to 1. So if the integral converges at all, the integrand is bounded and we are back to the situation of the previous paragraph with  $W(t) > 0$  and having a positive lower bound. In the contrary case,  $V = 0$  and  $m = 0$  or 1, the situation is more delicate but the sign question is absorbed into the issue of the physical meaning of surface divergences.

In summary, for all *finite* terms we have good control over the sign. (The  $\langle \Delta T_{00} \rangle$  terms are irrelevant to total energy, as discussed below.) One understands why Ambjørn and Wolfram [2, Table I] found nontrivial signs only for Dirichlet problems (not periodic or Neumann), and the particular sign patterns they saw are not surprising.

To understand the significance of various paths, it is useful to refine the classification of paths in the previous section. Each closed path is characterized by its image indices,  $j$  and  $k$ , and by its periodicity type, P, V, H, or C.

**P:** Periodic paths, producing constant terms in the energy density

**PZ:**  $j = 0 = k$  — the zero-length path

**PV:**  $j = 0, k \neq 0$  — vertical periodic paths

**PH:**  $k = 0, j \neq 0$  — horizontal periodic paths

- PD:**  $j \neq 0, k \neq 0$  — diagonal periodic paths
- V:** Nonperiodic closed paths whose uncompensated “bounce” occurs on the top or bottom side of the rectangle, producing energy densities depending on  $y$  only
- VP:**  $j = 0$  — perpendicular vertical bounce paths
- VD:**  $j \neq 0$  — vertical bounce paths with horizontal periodic drift
- H:** Nonperiodic closed paths whose uncompensated “bounce” occurs on the right or left side of the rectangle, producing energy densities depending on  $x$  only
- HP:**  $k = 0$  — perpendicular horizontal bounce paths
- HD:**  $k \neq 0$  — horizontal bounce paths with vertical periodic drift
- C:** Closed paths that are periodic in neither dimension, producing energy densities associated with corner images

Path PZ produces, by (17), the ubiquitous volume (here area) divergence,

$$T_{\text{PZ}}(t) = \frac{ab}{2\pi t^2}, \quad \langle E \rangle_{t\text{PZ}} = \frac{ab}{2\pi t^3}, \quad (64)$$

which, being ubiquitous, is always ignored (except for possible relevance to cosmological dark energy). All other terms in the energy density are pointwise finite, but some of them have nonintegrable divergences at the boundary. The path classes involved are VP and HP, which produce the well known surface (here perimeter) divergence in the total energy, and C, which produces an energy density that seemingly diverges at the corners but nevertheless makes no contribution to the “renormalized” total energy, as we shall see.

### 3.2 Energy calculations

Let us first dispose of  $\iint \langle \Delta T_{00} \rangle dx dy$ , which is expected to be zero because  $\Delta T_{00}$  is the divergence of a vector field, proportional to  $\phi \nabla \phi$ , that vanishes on every Dirichlet or Neumann boundary. From (41) and (43) we see that the quantity is indeed zero for periodic paths, while for corner paths it is proportional to the  $T_{00}(\frac{1}{4})$  term (which also will turn out to be zero). The situation for side paths is more subtle. The integral of  $\langle \Delta T_{00} \rangle_{tVjk}$  from (46) is not zero, which is not surprising since the field from a single image source does not satisfy the boundary conditions. However, because (46) is a total derivative, a calculation almost identical to that in (79)–(80) below shows that the sum over  $k$  does telescope to 0, at least when the top and bottom boundaries are of the same type (both Dirichlet or both Neumann).

The total energy contributed by a periodic path is trivially obtained by multiplying (40) by the area,  $ab$ . The sum of all such terms splits into PV, PH, and PD parts as

$$\begin{aligned} \langle E \rangle_{tP \setminus Z} = & -\frac{ab}{2\pi} \sum_{k=1}^{\infty} (-1)^{\eta} \frac{(2kb)^2 - 2t^2}{[t^2 + (2kb)^2]^{5/2}} - \frac{ab}{2\pi} \sum_{j=1}^{\infty} (-1)^{\eta} \frac{(2ja)^2 - 2t^2}{[t^2 + (2ja)^2]^{5/2}} \\ & - \frac{ab}{\pi} \sum_{j=1}^{\infty} \sum_{k=1}^{\infty} (-1)^{\eta} \frac{(2ja)^2 + (2kb)^2 - 2t^2}{[t^2 + (2ja)^2 + (2kb)^2]^{5/2}}. \end{aligned} \quad (65)$$

If all four sides are of the same type, (65) simplifies in the limit  $t \rightarrow 0$  to

$$\langle E \rangle_{tP \setminus Z} = -\frac{\zeta(3)a}{16\pi b^2} - \frac{\zeta(3)b}{16\pi a^2} - \frac{ab}{8\pi} \sum_{j=1}^{\infty} \sum_{k=1}^{\infty} (a^2 j^2 + b^2 k^2)^{-3/2} \quad (66)$$

(a well known result — e.g., [7]). In the special case of a square of side  $a$ , numerical evaluation of (66) gives  $-0.089859/a$  (identifiable with the vacuum energy of a torus of dimension  $2a$  as recorded in [2,7]). Because of the need to sum over a two-dimensional lattice, the numerical convergence is rather slow, even when repetitions of primitive orbits are handled all at once — in contrast with the situation for parallel plates, where the sum over paths has been found to be very efficient and increasingly so in higher dimensions [16,46].

To calculate the other  $T_{00}(\frac{1}{4})$  terms it is convenient to return to the cylinder kernel  $T$  and integrate it over the rectangle before taking the final  $t$  derivative in (25).

Consider first the paths of subclass VP. According to (44) with  $\mathbf{r}' = \mathbf{r}$ , for any path of class V we have

$$T_{Vjk}(t, \mathbf{r}, \mathbf{r}) = +\frac{(-1)^{\eta}}{2\pi} t [t^2 + (2ja)^2 + (2kb - 2y)^2]^{-3/2}. \quad (67)$$

Setting  $j = 0$  we arrive at

$$\int_0^a dx \int_0^b dy T_{V0k}(t, \mathbf{r}, \mathbf{r}) = \frac{(-1)^{\eta}}{2\pi} at \int_0^b [t^2 + (2kb - 2y)^2]^{-3/2} dy.$$

The terms with  $k = 0$  and  $k = 1$  are divergent (when  $t \rightarrow 0$ ) at the bottom and top boundaries, respectively. The other cases are finite, but need to be added to the divergent ones to build up a “clean” divergence, proportional to a power of  $t$ , that can be discarded in a systematic renormalization of the mass of the boundary plate. (Formally, this quantity is the total energy of an isolated

surface in otherwise empty space [3].) Again we consider for simplicity only the case where both horizontal boundaries are the same type, so that  $(-1)^\eta$  is independent of  $k$ . As a reminder that this assumption is in force, we shall write in resulting formulas

$$(-1)^\eta = \mp \equiv \begin{cases} -1, & \text{Dirichlet,} \\ +1, & \text{Neumann.} \end{cases} \quad (68)$$

The terms combine easily (telescope):

$$\sum_{k=-\infty}^{\infty} \int_0^a dx \int_0^b dy T_{V0k}(t, \mathbf{r}, \mathbf{r}) = \mp \frac{at}{\pi} \int_0^\infty (t^2 + 4y^2)^{-3/2} dy = \mp \frac{a}{2\pi t}.$$

Obviously the formula for class HP is the same with  $a$  replaced by  $b$ . Therefore, the total contribution from VP and HP to the trace of the cylinder kernel can be written as

$$T_\perp(t) = \mp \frac{P}{4\pi t}, \quad (69)$$

where  $P$  is the perimeter of the rectangle. It corresponds to a divergent surface energy

$$\langle E \rangle_{t\perp} = \mp \frac{P}{8\pi t^2}. \quad (70)$$

For paths of class VD we obtain

$$\sum_{k=-\infty}^{\infty} \int_0^a dx \int_0^b dy T_{Vjk}(t, \mathbf{r}, \mathbf{r}) = \mp \frac{at}{2\pi} \frac{1}{t^2 + (2ja)^2} = \mp \frac{t}{8\pi a j^2} + O\left(\frac{t^3}{j^4}\right).$$

The sum over  $j$  gives the well known  $\zeta(2)$ , so

$$\sum_{j \neq 0} \sum_{k=-\infty}^{\infty} \int_0^a dx \int_0^b dy T_{Vjk}(t, \mathbf{r}, \mathbf{r}) = \mp \frac{\pi t}{24a} + O(t^3).$$

The corresponding contribution to the energy is  $\pm\pi/48a$ ; it may be thought of as a Casimir correction to the surface energy of the sides at  $y = 0$  and  $y = b$  caused by the presence of the perpendicular sides with separation  $a$ . Thus the total energy from VD and HD paths is (at  $t = 0$ )

$$\langle E \rangle_{tD} = \pm \frac{\pi}{48} \left( \frac{1}{a} + \frac{1}{b} \right). \quad (71)$$

It is comparable in magnitude to the term from periodic paths, (66). In fact, for the square it is larger, since  $\pi/24 \approx 0.13$ ; that is why the “renormalized” (Lukosz) energy of the Dirichlet square comes out positive. (The situation for the *force* is different, however, as we shall see.)

Finally, for a path of class C we have from (42)

$$T_{Cjk}(t, \mathbf{r}, \mathbf{r}) = \frac{(-1)^\eta}{2\pi} t \left[ t^2 + (2ja - 2x)^2 + (2kb - 2y)^2 \right]^{-3/2}. \quad (72)$$

Terms with  $\{j, k\} \subset \{0, 1\}$  yield divergent integrals in the energy ( $\sim \int r^{-3} r dr$ ) if  $t$  is set equal to 0, but if one integrates with  $t$  positive, the result is quite different. We assume that all sides are of the same type, so that  $(-1)^\eta = +1$ . Then the contribution to the cylinder trace from the corner paths telescopes to

$$\begin{aligned} \sum_{j=-\infty}^{\infty} \sum_{k=-\infty}^{\infty} \int_0^a dx \int_0^b dy T_{Cjk}(t, \mathbf{r}, \mathbf{r}) &= \frac{2t}{\pi} \int_0^{\infty} dx \int_0^{\infty} dy (t^2 + 4x^2 + 4y^2)^{-3/2} \\ &= \frac{1}{4}. \end{aligned} \quad (73)$$

Being independent of  $t$ , this term makes no contribution at all to the energy via (30). (In a related independent calculation by Zaheer et al. [33] the corner paths were not even considered, because the rectangle was obtained as a limiting case of a configuration where they did not exist.) In the next subsection we shall review why this result is exactly what should have been expected.

### 3.3 Relation to heat kernel asymptotics

Let  $K(t, \mathbf{r}, \mathbf{r}')$  be the heat kernel corresponding to the system under study ( $\langle \mathbf{r} | e^{-tH} | \mathbf{r}' \rangle$  in quantum-mechanical notation, as contrasted with (15)). Let  $K(t)$  be its trace (cf. (17)). It is well known [47,48,49,8] that as  $t \rightarrow 0$

$$K(t) = \frac{A}{4\pi t} \mp \frac{P}{8\sqrt{\pi t}} + \frac{1}{4} + O(t^\infty), \quad (74)$$

where  $A = ab$  and  $P = 2(a+b)$  are the area and perimeter of the rectangle, and  $\mp$  is as in (68). (Here we state (74) only for the cases where all four sides are of the same type. The other cases — in which, for instance, the second term is not proportional to  $P$ , but the qualitative conclusions of this subsection remain true — are discussed in [50].)

It follows [23,51] that the trace of the *cylinder* kernel must have the expansion

$$T(t) = \frac{A}{2\pi t^2} \mp \frac{P}{4\pi t} + \frac{1}{4} + O(t), \quad (75)$$

and hence by (17) the regularized Casimir energy is

$$E(t) \equiv -\frac{1}{2} \frac{\partial T}{\partial t} = \frac{A}{2\pi t^3} \mp \frac{P}{8\pi t^2} + \frac{0}{t} + E_{\text{ren}} + O(t), \quad (76)$$

where  $E_{\text{ren}}$  is a constant traditionally identified as the “renormalized” Casimir energy. ( $E_{\text{ren}}$  is not determined by the heat kernel expansion (74); it is hidden in the  $O(t^\infty)$  term there.)

Our calculations above have confirmed (75) and (76) and determined  $E_{\text{ren}}$ . The terms in (75) are (64), (69), and (73).  $E_{\text{ren}}$  is the sum of (66) and (71) (in agreement with previous authors, including [2,27,33]).

With regard to the inevitability of the disappearance of the corner energy (without an explicit renormalization of any kind!), we stress [23,51] that the coefficient of  $1/t$  in (76) *must* be 0. (For dimensional reasons, that is where a corner term would need to appear, along with contributions linear in boundary curvature or in a Robin constant.) A  $t^{-1}$  term in  $E(t)$  would have to come from a  $\ln t$  term in  $T(t)$ , which in turn would be associated with a logarithmic term in  $K(t)$ , and such terms do not exist. On the other hand, there is no general reason why  $E(t)$  could not contain a  $\ln t$  term (and a resulting scale ambiguity in the “renormalization”). That would correspond to a  $t \ln t$  in  $T(t)$  and hence a  $t^{1/2}$  in  $K(t)$  — which can actually occur (for example in a disk), but does not in the model under study here.

### 3.4 Force and pressure calculations

We now investigate the force on the side at  $x = a$  from the field vacuum inside the rectangle, in the case where all sides are Dirichlet. From the previous subsections, the naively renormalized energy yields the force

$$-\frac{\partial E_{\text{ren}}}{\partial a} = +\frac{\zeta(3)}{16\pi b^2} - \frac{\zeta(3)b}{8\pi a^3} + \frac{b}{8\pi} \sum_{j,k=1}^{\infty} \frac{k^2 b^2 - 2j^2 a^2}{(j^2 a^2 + k^2 b^2)^{5/2}} + \frac{\pi}{48a^2} + 0, \quad (77)$$

where the terms are the contributions of path classes PV, PH, PD, VD, and HD, respectively.

It is important to remember that positive energy is not always the same thing as positive (repulsive) force, although that is true in many of the classic Casimir-force calculations in which the absolute value of the energy, being a negative power, decreases monotonically to 0 as the relevant geometrical parameter increases. In (77) the PV force is positive although the PV energy is negative; the individual terms in the PD force can have either sign, although their energies are all negative; the HD force is zero because the positive HD energy is independent of  $a$ . Piston analyses center on the cancellation of the positive PV force by an external force, since the sum of the other three terms can be shown to be negative (see Sec. 4).

As a first step toward less naive renormalization, one can keep the cutoff  $t$  finite and retain the cutoff-dependent terms in (76). Then the VP term produces a force

$$F_{tVP} = + \frac{1}{4\pi t^2}, \quad (78)$$

and the terms in (77) are modified in ways that can become significant when  $a$  or  $b$  is not large compared to  $t$ .

Another way to calculate the force is to integrate  $\langle T_{11}(a, y) \rangle$  over the side of the box. We take a moment to verify that the methods are consistent, using the appropriate formulas from Sec. 2.3.

*Periodic paths:* Multiplying (48) by  $b$  to perform the trivial integration, we get (after  $t \rightarrow 0$ )

$$F_{Pjk} = \frac{b}{4\pi} \frac{-2(2ja)^2 + (2kb)^2}{[(2ja)^2 + (2kb)^2]^{5/2}}.$$

Here  $j$  and  $k$  are not both 0; the terms with one, the other, or neither 0 add up to the first three terms in (77), as expected.

*Corner paths:* From the energy calculation we know that these terms should be zero. Also, from (51) we have  $T_{11} = 0$  unless  $\beta \equiv \xi - \frac{1}{4}$  is nonzero. For the  $\beta$  term (52), note that the integrand has the form of a total derivative,

$$\frac{K - 2(2bk - 2y)^2}{[K + (2bk - 2y)^2]^{5/2}} = \frac{d}{dy} \frac{y - bk}{[K + (2bk - 2y)^2]^{3/2}}. \quad (79)$$

Setting  $x = a$  and integrating over  $y$ , one gets

$$F_{tCjk} = - \frac{\beta}{\pi} \left\{ \frac{(1 - k)b}{[t^2 + 4(j - 1)^2 a^2 + 4b^2(k - 1)^2]^{3/2}} \right.$$

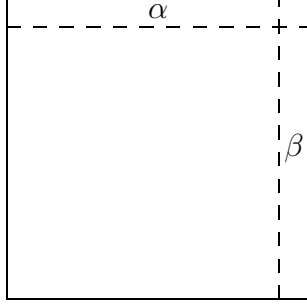


Fig. 5. Two regions where divergent surface energy appears.

$$- \left. \frac{(-k)b}{[t^2 + 4(j-1)^2 a^2 + 4b^2 k^2]^{3/2}} \right\}. \quad (80)$$

The sum of (80) over  $k$  from  $-\infty$  to  $\infty$  telescopes to 0.

*Side paths:* The class of paths that bounce off the side in question (along with an even number of additional reflections) have  $T_{11}$  identically zero (57). This is so even though the shortest such paths (those with  $k = 0$ ,  $j = 1$ ) give rise to a divergent energy in the region marked  $\beta$  in Fig. 5. This matches the 0 in (77).

Much more interesting are the paths that bounce off the horizontal walls. From (54)–(55),

$$\begin{aligned} \langle T_{11} \rangle_{tVjk} = & -\frac{1}{4\pi} [t^2 + (2ja)^2 + (2kb - 2y)^2]^{-5/2} [t^2 - 2(2ja)^2 + (2kb - 2y)^2] \\ & + \frac{\beta}{\pi} [t^2 + (2ja)^2 + (2kb - 2y)^2]^{-5/2} [t^2 + (2ja)^2 - 2(2kb - 2y)^2]. \end{aligned}$$

For fixed  $j, k$  the  $\beta$  term is just like the corresponding corner term with  $j - 1$  replaced by  $j$  and the sign changed. Therefore, these two classes of  $\beta$  terms would cancel when summed over  $j$ , even if they did not vanish when summed over  $k$  as we just saw.

It remains to integrate the other part of  $\langle T_{11} \rangle_{tVjk}$  over  $y$  from 0 to  $b$ . The terms with  $j = 0$  lead to a clone of the calculation following (67). In particular, those terms for which also  $k = 0$  or 1 are divergent when  $t \rightarrow 0$ . This divergent pressure clearly corresponds, in the case  $k = 1$ , to the divergent energy in region  $\alpha$  associated with paths VP that bounce perpendicularly off the top boundary. (From  $k = 0$  comes a corresponding effect at the bottom boundary, not indicated in Fig. 5.) That energy is proportional to the length of the box and hence gives a force (78) upon differentiation.

Finally, one wants to integrate the terms with  $j \neq 0$  and see that they reproduce the remaining (VD) term in (77). The integral of each term is, at



$t = 0$ ,

$$-\frac{1}{4\pi} \frac{\frac{b[32a^4j^4+16a^2b^2j^2(k-1)^2](k-1)}{[4a^2j^2+4b^2(k-1)^2]^{3/2}} - \frac{bk[32a^4j^4+16a^2b^2j^2k^2]}{[4a^2j^2+4b^2k^2]^{3/2}}}{16a^4j^4}.$$

At first glance it may seem that this expression sums over  $k$  to zero, by the same telescoping argument used elsewhere. However, unlike those previous sums, in this case the individual terms do not approach 0 as  $|k| \rightarrow \infty$ ; rather, they go to  $1/(32\pi a^2 j^2)$ . Taking account of both signs of  $k$  and  $j$ , one gets the force to be

$$F_{\text{VD}} = 4 \sum_{j=1}^{\infty} \frac{1}{32\pi a^2 j^2} = \frac{\zeta(2)}{8\pi a^2} = \frac{\pi}{48a^2},$$

as needed.

Although this exercise may appear redundant, it has underscored two important points. First, doing the calculation in terms of pressure instead of energy by no means eliminates the problem of divergences. Second, the divergent pressure on a given wall is not associated with the divergent energy adjacent to the wall (in region  $\beta$  in Fig. 5). Rather, it goes with the divergent energy adjacent to the intersecting perpendicular walls (such as in region  $\alpha$ ).

## 4 The Casimir piston

The physical significance of the forces calculated in [1], in our Sec. 3.4, and in much intervening literature has been called into question. For one thing, unlike the celebrated sphere calculations of Boyer [52] and others, these calculations are unable to take into account any forces coming from the region outside the box. In addition, within the framework of ultraviolet-cutoff regularization the uncompensated divergent energy proportional to the surface area cannot be easily dismissed in deducing the force conjugate to a dimension whose variation changes the surface area. In our case the offending energy is that localized in the region  $\alpha$  in Fig. 5, which is proportional to the length of the box, and the corresponding pressure was also observed in Sec. 3.4 in the direct calculation of  $\langle T_{11} \rangle$  on the movable side of the box.

Cavalcanti [27] proposed to avoid both problems by considering a different situation, the piston (Fig. 6). The interior partition is free to move horizontally, and one is to calculate the force upon it.  $L$  is to be taken very large compared to  $a$  and  $b$ . The argument now is that the exterior of the apparatus is unchanging and hence irrelevant to the force, whereas both interior chambers

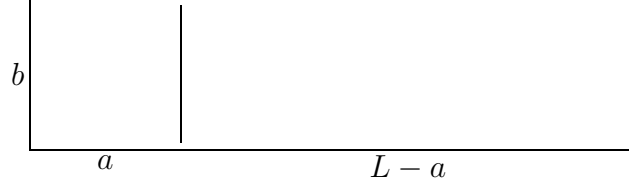


Fig. 6. A rectangular piston in dimension 2. Its “shaft” has length  $L - a$ , effectively infinite. The word “piston” refers both to the movable plate at  $x = a$  and to the model as a whole.

can be treated exactly. Furthermore, the total of the interior side lengths is independent of the piston position,  $a$ , so that the surface divergences cancel in the calculation of the force.

Generalizations and variations of this model have been extensively studied [28,29,30,53,54,55,56,57,58,59,60,61,62].

The piston model is not without its own physical problems, because interactions between the piston plate and the horizontal sides have been ignored. In a realistic experiment, because of ordinary Casimir attraction the plate would be unstable to striking the tube wall on edge, after which it would collapse against one of the walls of the tube. It may be argued that this objection is irrelevant to the question of principle that the piston model is designed to address; the only degree of freedom one is varying is  $a$ , so it is legitimate to imagine that the plate is constrained from moving in any other degree of freedom. There still exists a Casimir force between the plate and the nearest wall, though it is somehow prevented from causing motion. However, one can argue by symmetry that this force has no significant horizontal component, so that the piston theorists are justified in ignoring it. Nevertheless, in a real apparatus there would surely be some friction with the walls, so the feasibility of an experiment to verify the piston analysis is questionable.

Putting these doubts aside, we summarize and recast the Cavalcanti analysis in our framework of closed paths. The finite part of the force on the piston from the chamber on the left has been calculated in (77). The force coming from the shaft on the right can be found from the same formula, with the sign reversed,  $a$  replaced by  $L - a$ , and  $L$  taken to infinity; the only term that survives is the PV term,

$$F_L = -\frac{\zeta(3)}{16\pi b^2}. \quad (81)$$

It exactly cancels the corresponding term in (77), leaving PH, PD, and VD terms:

$$F_{\text{pist}} = -\frac{\zeta(3)b}{8\pi a^3} + \frac{b}{8\pi} \sum_{j,k=1}^{\infty} \frac{k^2 b^2 - 2j^2 a^2}{(j^2 a^2 + k^2 b^2)^{5/2}} + \frac{\pi}{48a^2}. \quad (82)$$

Here there is no “naive renormalization” as in (77), since the divergences (in particular, the VP terms) would explicitly cancel if the calculation were done for the complete piston before removing the cutoff.

Cavalcanti [27] rendered (82) more illuminating by subjecting it to further analysis. If one refrains from the  $\zeta(3)$  simplification, the complete sum over periodic paths in the ( $t = 0$ ) energy, (66), is

$$\langle E \rangle_{tP \setminus Z} = -\frac{ab}{32\pi} \sum_{\substack{j,k=-\infty \\ (j,k) \neq (0,0)}}^{\infty} (j^2 a^2 + k^2 b^2)^{-3/2}. \quad (83)$$

From this one can derive two complementary formulas, useful in the respective regimes  $a \gg b$  and  $a \ll b$ . (Unfortunately, none of the three formulas for  $F_{\text{pist}}$  is completely transparent for  $a \approx b$ .)

In the first case, for  $j = 0$  one evaluates the  $k$  sum to the term PV (the first term in (66)), as before, but for fixed  $j \neq 0$ , one applies a known relation between the  $k$  sum (which is an Epstein zeta function) and a series of modified Bessel functions. (This theorem traces back ultimately to the Poisson summation formula; see the appendices of [2] and [8].) Thus the PH and PD terms together are replaced by the energy terms

$$-\frac{\pi}{48a} - \frac{1}{2b} \sum_{j,k=1}^{\infty} \frac{k}{j} K_1 \left( 2\pi j k \frac{a}{b} \right).$$

(The individual terms in the sum cannot be associated with individual periodic orbits, nor with individual eigenvalues.) Remarkably, the first term of this expression precisely cancels the VD term, so that PH, PD, and VD all together reduce to the energy

$$-\frac{1}{2b} \sum_{j,k=1}^{\infty} \frac{k}{j} K_1 \left( 2\pi j k \frac{a}{b} \right).$$

Since HD does not contribute to the force and the PV force is still cancelled by the force from the shaft, the force on the piston is [27, (11)]

$$F_{\text{pist}} = \frac{\pi}{b^2} \sum_{j,k=1}^{\infty} k^2 K_1' \left( 2\pi j k \frac{a}{b} \right). \quad (84)$$

It follows that the piston force (a) is always negative, (b) vanishes exponentially fast for  $a \gg b$ , in contrast to the usual power-law decay of the Casimir force.

Alternatively, one can apply the Epstein-to-Bessel transformation to the  $j$  sum

for fixed  $k$ . That is, PV and PD get replaced by

$$-\frac{\pi}{48b} - \frac{1}{2a} \sum_{j,k=1}^{\infty} \frac{k}{j} K_1 \left( 2\pi j k \frac{b}{a} \right).$$

The first term cancels HD (which doesn't contribute to the force anyway); the VD term remains (as does PH); and the PV term has been absorbed, so that the force from outside the piston is now uncompensated. Thus the total force on the piston is [27, (14)]

$$F_{\text{pist}} = -\frac{\zeta(3)b}{8\pi a^3} + \frac{\pi}{48a^2} - \frac{\zeta(3)}{16\pi b^2} + \frac{\pi b}{a^3} \sum_{j,k=1}^{\infty} k^2 K_0 \left( 2\pi j k \frac{b}{a} \right). \quad (85)$$

As Cavalcanti explains, this form is nicely adapted to understanding the regime  $a \ll b$ , where the standard Casimir result is, of course, recovered in the limit.

Energy is fungible, so one must beware of attributing too fundamental a connection between particular classes of paths and the observable net forces. The striking thing is that the calculations reveal several exact cancellations, not all of which can be implemented at the same time.

## 5 The Casimir pistol

The Casimir piston has proved to be a highly illuminating model, but it does not settle the issue of the true physical significance of the purely internal vacuum pressure on the side of a rectangular cavity. In the piston both the divergent (VP) and the positive finite (PV) internal pressure are exactly balanced by the precisely analogous pressures in the long shaft on the other side of the movable plate. This observation does not tell us what would happen if the external shaft were not there. The problem of real interest is a rectangular box with one side free to move, as indicated schematically in Fig. 5 and more realistically in Fig. 7. The main question is whether the force on the movable side is attractive or repulsive. This is a question about disjoint rigid bodies, so it is a meaningful physical problem, just like the piston. (The 3D electromagnetic case should be qualitatively similar to the 2D scalar problem.) Another urgent question is what happens to the VP divergence now that there are no VP paths in the shaft to compensate it; the previous paradox (Sec. 3) of an apparent infinite pressure has reappeared.

The problem is difficult because there is no reliable analytical calculation of the forces acting from outside the box and inside the tiny gaps at the ends of the lid. If we momentarily ignore the gaps, it seems unlikely that the external

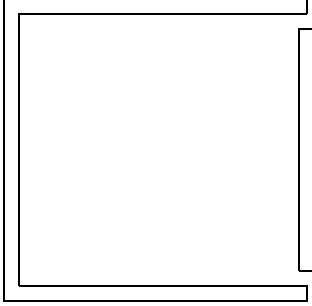


Fig. 7. A rectangular box with one side (“lid”) free to move. The box has walls of finite width and a finite gap between the lid and the box sides.

forces would be very large (although we find unconvincing Lukosz’s attempt [1] to prove this fact by appealing to Weyl’s theorem). If one thinks in terms of closed paths, paths striking the walls perpendicularly will yield only the usual surface divergence, so the only possible source of nontrivial external forces is the diffractive paths striking the corners. If this diffractive effect is small, therefore, one might expect the force to be repulsive when the plate is exactly at the mouth of the box. However, if the plate is located significantly inside or outside the box, intuition says the opposite: “inside” we are getting into the piston regime, whereas “outside” the Casimir attraction between the nearest neighboring regions of the two bodies should be dominant.

A convincing resolution of this apparent paradox presumably requires a serious study of the gap region in a less idealized geometry, as in Fig. 7. It is clear that what happens around the gap is very complicated, especially when the plate is part-in and part-out as in that figure. One should note that the symmetry argument used in Sec. 4 to dismiss the forces in the gap is no longer applicable.

The uncertainty about the external and gap forces is somewhat alleviated if we replace the thin lid by a large rectangular object (Fig. 8). The piston plate has now become more like a bullet or artillery shell. The question now is the sign of the force for various values of the five dimensions indicated in Fig. 8: Does a Casimir pistol exist? The advantage of this new problem is that the corners of the two bodies are not near each other, so there are no short classical paths outside the apparatus (as long as neither  $d$  nor  $e - d$  is small), even if diffractive paths are admitted as classical. (One could eliminate diffractive paths (in the sense we are using the term) by replacing the barrel and bullet by similarly shaped objects with smooth boundaries.) Like all piston authors, we continue to consider only horizontal motion (variation of  $a$ ) and therefore ignore the vertical force between the bullet and the shaft of the barrel.

We now consider the implications of taking the small gap of width  $c$  seriously. (We speak only of the gap at the top, but obviously the same remarks apply to the one at the bottom.) The first (and motivating) observation is that the total side length of the system is now fixed, and hence so is the transverse

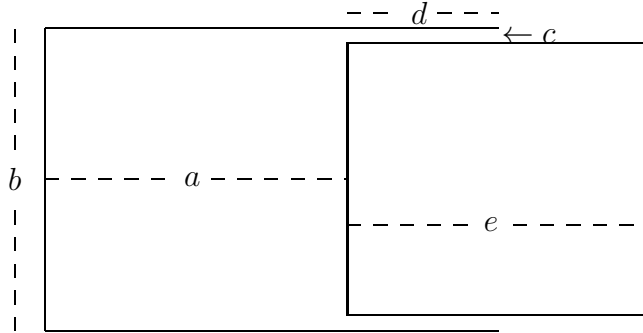


Fig. 8. The Casimir pistol, consisting of two disjoint, perfectly conducting bodies, the barrel and the bullet. It is shown schematically, as in Fig. 5, but the barrel can be thought of as having finite thickness, as in Fig. 7.

extent of the infinite (or cutoff-dependent) surface energy. In particular, the energy associated with what we call VP paths (including those striking the exterior of the apparatus) is independent of  $a$ . The associated paradox is thereby removed!

Our joy in this victory should be short-lived, however. If we take VP paths inside the gap seriously, then for consistency we must also take PV paths across the gap seriously, and we shall see that they present a serious problem.

Nonperpendicular paths inside the gap eventually escape from it, so they are not “short” and probably can be neglected. (In the model of [33], all such paths escape to infinity and hence can never be closed. In our case it is possible, but rare, for such a path to bounce off the left side of the rectangle and return to its starting point.) From the point of view of a point  $\mathbf{r}$  inside the rectangular region of area  $ab$ , the box now has small “leaks” of width  $c$ , but one would not expect that to affect its internal Casimir energy significantly. This observation could be made quantitative by imitating a calculation in [33], but we shall not do so here, because we are interested only in the limit of very small  $c$ .

On the other hand, because the gap  $c$  is much smaller than the box dimensions,  $a$  and  $b$ , the Casimir energy associated with the rectangle of area  $cd$  is much greater than that of the box. The principal force associated with this gap rectangle is the vertical Casimir attraction between the bullet and the barrel, but we have agreed to impose a constraint that makes it irrelevant. However, it is the very essence of the piston argument, especially as developed by Hertzberg et al. [29,30], that the proportionality of the Casimir energy to  $d$  produces a horizontal force, independent of  $d$  but proportional to  $1/c^2$ . (This energy is precisely the contribution of the vertical periodic (PV) paths.) In the present scenario this force has sign opposite to the Lukosz force in the box, because  $d$  increases when  $a$  decreases, and a larger magnitude than the analogous force in the piston scenario, because  $c < b$ . Therefore, if we accept all the approximations involved in this argument, we are forced to the conclusion

that the bullet is sucked into the barrel, not expelled from it.

Let us list those assumptions.

- (1) The gap between the bullet and the barrel does not significantly affect the Lukosz force from the empty part of the pistol chamber.
- (2) There are no significant forces from outside the pistol.
- (3) The effect of the gap can be estimated by ignoring nonperpendicular paths and treating the perpendicular paths as usual, as if we had simply a pair of parallel plates there.

Obviously, a trustworthy treatment of this system requires either a numerical analysis (for example, by the method of Gies et al. [63]) or, better still, a breakthrough in the analytical treatment of convex corners. As a positive result in this direction, we report that it is possible to compute exact forces and torques between bodies of arbitrary shape in weak coupling (for example, materials with dielectric constant nearly unity). For example, two thin parallel plates of finite length experience an attractive lateral force that tends to cause the plates to move to a configuration where they are centered on each other. This is the attractive force that tends to increase the length of the gap in the pistol. (A recent independent investigation [64] likewise shows a system maximizing the length of a small gap between flat surfaces.) Moreover, in addition to the attractive force between the plates, there is a torque exerted on one thin plate above a larger plate which tends to cause a rotation of the smaller plate about its center of mass so as to favor perpendicular orientation. Details have been reported in [39,40]. Since these qualitative conclusions are essentially geometrical, they should also hold for strong coupling (Dirichlet boundary conditions).

Finally, let us try to confirm the foregoing conclusions by looking at pressure integrals. In principle, one can find the total force on the bullet by integrating the appropriate components of  $\langle T_{\mu\nu} \rangle$  over the surface of the bullet (or even some larger surrounding surface [31,32]). The integral over the back side of the bullet is essentially the same as in Sec. 3 (apart from the “infinite” term). On the top and bottom sides, the relevant component is  $T_{12}$ , and a check of the formulas (49), (51), (56), (57) shows that the contributions all vanish. So, one would conclude that the pistol fires after all! We believe that the resolution of this new paradox is that the crude approximations listed above, although they *may* be permissible for the energy calculation, are simply wrong for the pressure calculation. In particular, if the Casimir (or the Lukosz) formulas were accurate over the entire gap rectangle, there would be finite jumps at the end surfaces of the gap in  $\langle T_{11} \rangle$  (which is constant and large in the gap, constant and smaller in the chamber, and zero in the exterior, in our approximations). By the conservation law, there is then a delta function (of  $x - (\text{endpoint})$ ) in  $\langle \partial T_{12} / \partial y \rangle$ . A more realistic calculation would smear out this singularity,

probably creating a lump of  $\langle T_{12} \rangle$  that decreases more or less linearly in  $y$  away from the back corner of the bullet and also downward away from the front edge of the barrel. These stress terms would create horizontal forces. They are very much like the stresses found in [31, Figures 4(d,e,f)].

## 6 The Casimir pistol with cutoff

### 6.1 Parallel plates revisited

Our discussion so far has concerned the 2D scalar analogue of the idealized perfect-conductor model of the interaction of the electromagnetic field with metal bodies. It is generally agreed that the divergences (except for the universal volume divergence) encountered in such calculations are the fault of the physical failure of that model at high frequencies — equivalently, at length scales so small that the material cannot be modeled as a continuum. It is also now agreed that the energy divergences, or the corresponding cutoff-dependent terms in a calculation with a cutoff, being independent of the bodies' positions, do not appear in the forces between rigid conducting bodies. It is sometimes forgotten that the idealized Casimir theory runs into physical trouble already for rigid bodies, even the canonical scenario of parallel flat plates, when the distances become too small. It predicts an energy per unit cross section,  $\mathcal{E}$ , proportional to  $-a^{-d}$  for plates with separation  $a$  in  $d$ -dimensional space. If taken literally, this says, implausibly, that  $\mathcal{E}$  becomes (negatively) infinite when  $a$  goes to zero. One would expect instead that in that limit  $\mathcal{E}$  approaches a constant, since then the space between the plates has disappeared and space is filled by the perfectly conducting material. (In fact, the constant should make the total energy turn out to be 0 when suitably defined surface energies are also taken into account.)

Barton [65] has done extensive calculations for dielectric bodies with a polarizability small enough to be treated perturbatively (the opposite regime from perfect conductivity). He showed (see also [66]) that a spatial cutoff at atomic distances serves to cure the divergences (which otherwise remain even in the usual model of quadratic falloff of dielectric constant with frequency — e.g., [67,68]). Roughly speaking, the mathematical effect of such a cutoff is similar to that of a very rapid, such as exponential, cutoff at high frequency. In Barton's theory the total energy per unit cross section does approach 0 as  $a \rightarrow 0$  when the surface energy is included. In this model, as  $a \rightarrow 0$  there is a constant attractive force proportional to the energy density of the uniform medium, no matter how the latter is regulated [69].

More recently, Barton [70,71] has developed a plasma model that is more



pertinent to the limit of perfect conductivity. It also involves an atomic-scale cutoff, but one affecting only the wavelengths parallel to the boundaries.

Our aim here is to stay in the highly conducting regime and to see whether keeping the exponential cutoff parameter  $t^{-1}$  finite, at some value typical of atomic separations, yields a physically plausible (and divergence-free) model of Casimir phenomena. Although ultimately no substitute for serious microscopic modeling of conductive materials (an unavoidably nonlinear problem), this approach offers hope of rescuing the huge investment that has been made into treating vacuum problems (relatively easily) by spectral analysis of linear partial differential operators. It also provides a route to understanding the gravitational significance of “divergent” local energies and stresses [42]. This cutoff should be regarded as analogous to the ad hoc repulsive core in the Lennard–Jones potential in atomic physics. A more accurate potential should be based on the electronic structure of the atoms; but one would not then apply such a potential to, say, nucleon-nucleon scattering. Similarly, a detailed theory of real metals is not relevant to hadron bags, cosmological branes, thermal fluctuations in soft-matter physics, and other systems where Casimir-like effects have been studied. Within our two-dimensional scalar model (which is pertinent to all these contexts, if to any) the simple exponential cutoff has the advantage of being universal, but we and readers must remain conscious that its relevance at small distances to any particular real physical system is qualitative at best. We stress again that this atomic-scale cutoff must not be confused with the well known decrease of dielectric constant with frequency above the plasma frequency; we make no attempt to model the latter, which is specific to the electromagnetic scenario.

In the context of the Casimir pistol, the idea is that the small gap  $c$  surrounding the bullet must be in the sub-Casimir regime if the other dimensions ( $a$ ,  $b$ ,  $d$ ) are in the regime where Casimir effects are significant, and, therefore, the deduction in Sec. 5 of a dominant attractive force originating in the gap goes outside the regime of validity of the theory. Although the cutoff theory has no fundamental physical justification, it is probably a bit closer to the truth. (Unfortunately, we shall see that no robust conclusion is attainable by this route.)

Maclay and Villarreal [72] proposed this same kind of cutoff and hence obtained formulas and graphs rather similar to ours in this section. However, they identified  $t$  with the reciprocal of the plasma frequency rather than, as we do, the interatomic spacing, which is typically 100 times smaller (again cf. [65]). Other authors [73,74] considered (for refutation) an even bigger exponential cutoff length, adequate to make the unrenormalized vacuum energy of empty space consistent with cosmological observations, and showed that such theories predict Casimir repulsion at distances large enough to be refuted by the existing laboratory experiments.

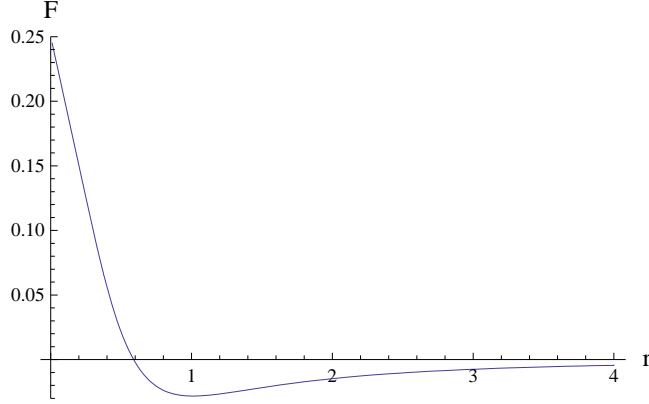


Fig. 9. Graph of  $F(r)$  as a function of  $r$ .

Before studying the pistol, let us look at the attraction between parallel plates with the cutoff retained. This could be done easily in any dimension, but for coherence in this paper we retain dimension 2. If the separation between plates is  $a$ , we take the  $b \gg a$  limit of (65), in which only the perpendicular paths ( $k = 0$ ) contribute, and divide by  $b$  to get energy per unit length:

$$\mathcal{E} = \frac{a}{\pi} \sum_{j=1}^{\infty} \frac{t^2 - 2j^2 a^2}{(t^2 + 4j^2 a^2)^{5/2}}. \quad (86)$$

This function behaves in keeping with the idea that the energy or the force should be damped when  $a$  is comparable to the nanoscale (interatomic spacing) represented by  $t$ . Of course, when  $a \gg t$ , the effect of  $t$  is negligible and (86) gives the standard result. It is convenient to measure  $a$  in units of  $t$ . If  $a = st$ , then  $\pi t^2 \mathcal{E} = F(s)$ , where

$$F(r) \equiv r \sum_{j=1}^{\infty} \frac{1 - 2j^2 r^2}{(1 + 4j^2 r^2)^{5/2}} \quad (87)$$

(see Fig. 9).  $F(r)$  has a zero at  $r_0 \approx 0.5888$ . It has a minimum (a zero of the force) at  $r_1 \approx 1.0105$ , with  $F(r_1) \approx -0.02821$ . At large  $r$ ,  $F(r) \sim -\zeta(3)/16r^2$  as in the theory without cutoff. For small  $r$  the Euler–Maclaurin formula [75, (23.1.30)] shows that  $F(r) \sim \frac{1}{4} - \frac{r}{2} + O(r^N)$  for arbitrarily large  $N$ . Thus  $F(0)$  precisely cancels the surface energy from (70) (where  $P = 2$  because we are looking at unit cross section on two plates), so that the total energy at  $s = 0$  is indeed 0. (But this result may be an accident. It does not happen for the Neumann boundary condition. Also, as we shall now observe,  $s = 0$  seems to represent material under compression, not a solid block of ordinary material.)

At  $r < r_1$  this model predicts a repulsion. Therefore, it must violate the hypotheses of the theorems stating that vacuum forces between symmetrical bodies separated by a plane are always attractive [76,77]. The argument of

Kenneth and Klich [76] refers to the standard dielectric model of the media, or a scalar analog thereof, into which our cutoff does not fit. The mathematical reason why the theorem of Bachas [77] doesn't apply is less clear, but the key physical point is clear from that author's remarks (p. 9094) that a "quantized particle does not, strictly speaking, live in one side of the reflecting plane," and that the theorem would apply at the quantum level only if (in the terms of our scenario) one of the slabs were made of antimatter. The repulsion occurs only at separations of the order of the interatomic spacing. Thus the model mocks up a more realistic theory in which the two slabs are not cleanly separated, in accordance with Barton's remark [65, p. 4088], "[A sharp short-distance cut-off,] though a fiction, is a convenient shortcut to somewhere near the truth. At small separations, overlap between the electron clouds makes the interatomic potential highly repulsive...." We recall also that Ford and Svaiter [21] found that a similar effect was induced by a stochastic uncertainty in the position of the conducting boundaries, which must in general lead to some probability of interpenetration. In short, nobody should be surprised to encounter a repulsion when pushing two slabs of material together. A normal, stable material must resist compression. Of course, such repulsion is not a "Casimir effect"; a quantitative study would require detailed modeling of the material, and it is a surprise and probably an accident that our crude field-theoretic model gives such plausible results in this regime. In particular, the fact that our potential minimum occurs at a small positive separation, rather than zero or negative, is not to be taken too seriously.

## 6.2 Energy in the pistol

Now we do the energy accounting for the pistol, under the three assumptions listed in Sec. 5. (The notation is a slight simplification of that in Sec. 3.)

*Energy in the chamber:* According to assumption (1), the contribution  $E_P$  of periodic paths is still given by (65) with  $\eta = 0$ . Corner paths can be ignored because they make no contribution to the total energy. HP and HD paths can be ignored here because they make no contribution to the relevant force (their energies being independent of  $a$ ). The contribution of VP paths is the  $a$ -dependent term of (70):

$$E_{VP} = -\frac{a}{4\pi t^2}. \quad (88)$$

The contribution of VD paths is given by the generalization of (71) to finite cutoff,

$$E_{VD} = \frac{a}{2\pi} \sum_{j=1}^{\infty} \frac{-t^2 + 4j^2 a^2}{(t^2 + 4j^2 a^2)^2}. \quad (89)$$

*Energy in the barrel:* In the formulas above,  $(a, b)$  must be replaced by  $(d, c)$ , and we must multiply by 2 to count both top and bottom gaps. In accordance with assumption (3), only vertical paths ( $j = 0$ ) will be considered. The PV paths give

$$E_{P'} = \frac{2cd}{\pi} \sum_{k=1}^{\infty} \frac{t^2 - 2k^2c^2}{(t^2 + 4k^2c^2)^{5/2}}. \quad (90)$$

The VP paths give

$$E_{VP'} = -\frac{d}{2\pi t^2}, \quad (91)$$

of which half belongs to the barrel and half to the bullet. As expected, the barrel part combines with (88),

$$E_{VP} + \frac{1}{2}E_{VP'} = -\frac{a+d}{4\pi t^2},$$

to yield something independent of  $a$ , because  $a+d$  is constant. Similarly, the bullet part of (91) combines with the surface energy of the part of the bullet outside the barrel.

*Summary of pistol energy:* The only energy terms that contribute to the force (under our assumptions) are

$$E = E_P + E_{VD} + E_{P'} \quad (92)$$

as listed above. We could differentiate with respect to  $-a$  (using  $\frac{\partial}{\partial d} = -\frac{\partial}{\partial a}$ ) to get the force. All the sums encountered can be expressed in terms of inhomogeneous Epstein zeta functions [6,8]. However, for our purposes it is better to analyze the various terms qualitatively. (Quantitatively, we claim nothing for the model at short distances anyway.)

### 6.3 Asymptotics and numerics for the pistol

Let  $c = rt$ ,  $a = st$ ,  $b = ut$ ,  $d = L - a = (l - s)t$  (see Fig. 10). We want to examine  $E$  as a function of  $s$ , with  $r$  of order unity and  $s, u, l - s$  much larger. From (92) and (65) we have

$$E = E_{PV} + E_{PH} + E_{PD} + E_{VD} + E_{P'}$$

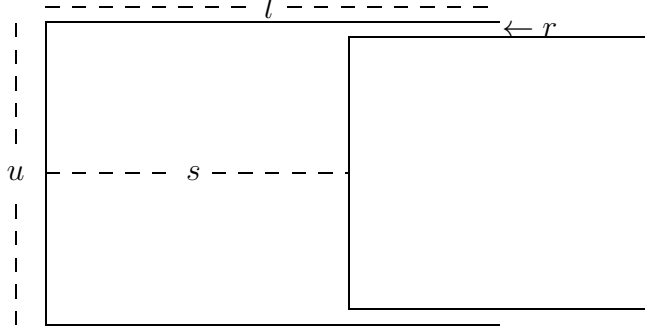


Fig. 10. Pistol dimensions in units of  $t$ .

$$\begin{aligned}
&\equiv \frac{us}{\pi t} \sum_{k=1}^{\infty} \frac{1 - 2k^2 u^2}{(1 + 4k^2 u^2)^{5/2}} + \frac{us}{\pi t} \sum_{j=1}^{\infty} \frac{1 - 2j^2 s^2}{(1 + 4j^2 s^2)^{5/2}} \\
&+ \frac{2us}{\pi t} \sum_{j=1}^{\infty} \sum_{k=1}^{\infty} \frac{1 - 2j^2 s^2 - 2k^2 u^2}{(1 + 4j^2 s^2 + 4k^2 u^2)^{5/2}} \\
&+ \frac{s}{2\pi t} \sum_{j=1}^{\infty} \frac{-1 + 4j^2 s^2}{(1 + 4j^2 s^2)^2} + \frac{2r(l-s)}{\pi t} \sum_{k=1}^{\infty} \frac{1 - 2k^2 r^2}{(1 + 4k^2 r^2)^{5/2}}. \tag{93}
\end{aligned}$$

Let  $E_{P''}$  denote the part of  $E_{P'}$  proportional to  $s$ . The other term in  $E_{P'}$  (proportional to  $l$ ) is independent of  $s$  and hence shall be ignored in further discussion of the force on the bullet (including Figs. 11–12).

The terms  $E_{PV}$  and  $E_{P''}$  are linear functions of  $s$ , while the other three terms are nonlinear. The linear terms dominate the force at large  $s$ , and the main point of interest is the confrontation of  $E_{P''}$  (Casimir energy in the gap) with  $E_{PV}$  (identified in Sec. 3.4 as the source of the Lukosz repulsive force; it is the term that would give an attractive Casimir force between the upper and lower walls of the chamber if those were allowed to move). We shall see that generically the  $P''$  term is dominant. At small  $s$  the nonlinear terms dominate and collectively give a function qualitatively similar to that in Fig. 9. Two cases are exhibited in Figs. 11 and 12.

In more detail, by approximating the sums by integrals one can show that (when the dimensions other than  $r$  are  $\gg 1$ )

$$\pi t E_{PH} \sim -\frac{\zeta(3)u}{16s^2} \Rightarrow \text{attractive force} \sim -\frac{C'u}{s^3}; \tag{94}$$

$$\pi t E_{VD} \sim +\frac{\zeta(2)}{8s} \Rightarrow \text{repulsive force} \sim +\frac{C}{s^2}; \tag{95}$$

$$\pi t E_{PD} \sim h\left(\frac{s}{u}\right) \frac{1}{u} \text{ for some function } h, \text{ such that}$$

$$s \gg u \gg 1 \Rightarrow \pi t E_{PD} \sim -\frac{\zeta(2)}{8s} \Rightarrow \text{attractive force} \sim -\frac{C}{s^2} \tag{96}$$

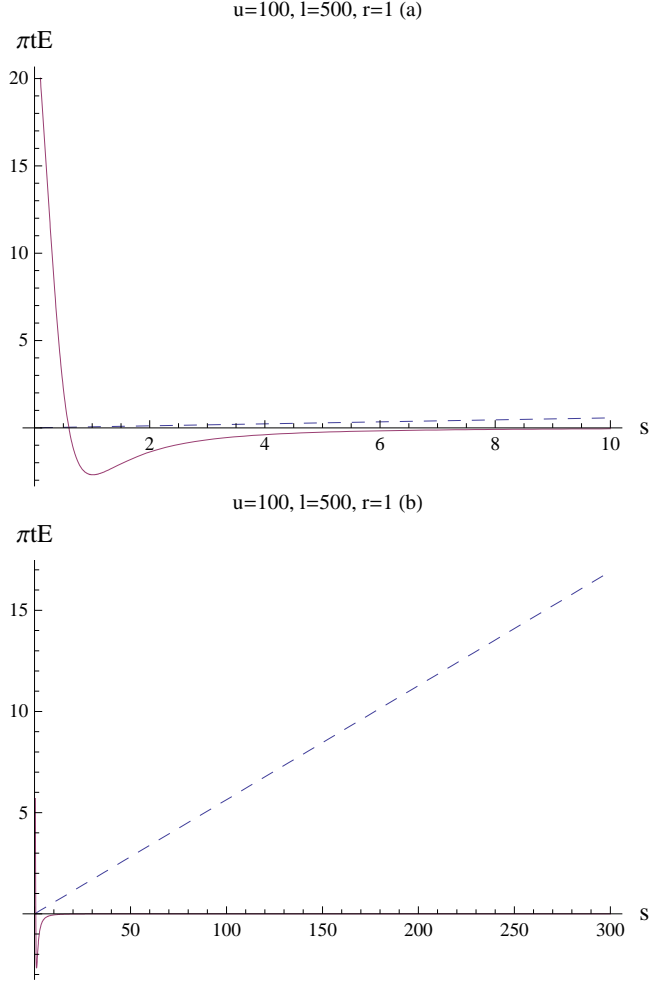


Fig. 11. Graphs of linear (dashed) and nonlinear (solid) parts of  $\pi t E(s)$  for  $r = 1$ ,  $u = 100$ ,  $l = 500$ . (a) Small  $s$ ; linear terms are negligible. (b) Large  $s$ ; linear terms dominate and create an attractive force.

so that  $E_{\text{VD}}$  and  $E_{\text{PD}}$  cancel to leading order in  $1/s$ , and

$$u \gg s \gg 1 \Rightarrow \pi t E_{\text{PD}} \sim -\frac{\zeta(2)}{8u} + O\left(\frac{s}{u^2}\right) \quad (97)$$

so that the PD force vanishes to leading order in  $1/u$ . In the regime  $u \gg s$  the PH force dominates the other nonlinear terms. (In the absence of fine tuning, it is still smaller than the linear term unless  $u \gg s^3$ .) In the small- $t$  limit (i.e.,  $s \gg 1$ ) the PH force reduces to the first term in (85), which is simply the standard Casimir force between the left chamber wall and the bullet, whereas for general  $s$  its energy is  $E_{\text{PH}} = uF(s)/\pi t$  — exactly proportional to the parallel-plate function in Fig. 9. Finally, for large  $s$  ( $s \gg u^{1/3}$ ) all the nonlinear forces are small compared to the linear ones, unless the latter happen to cancel.

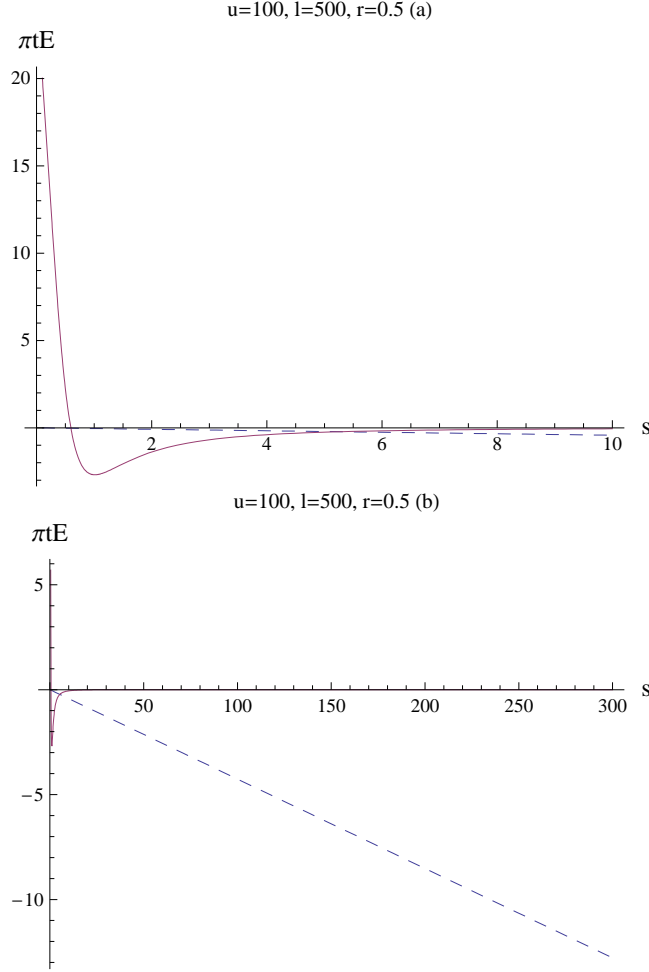


Fig. 12. Graphs of linear (dashed) and nonlinear (solid) parts of  $\pi t E(s)$  for  $r = 0.5$ ,  $u = 100$ ,  $l = 500$ . (a) Small  $s$ ; linear terms are negligible. (b) Large  $s$ ; linear terms dominate and create a repulsive force.

Indeed, the forces arising from the linear terms are

$$\pi t^2 F_{PV} = -F(u), \quad \pi t^2 F_{P''} = +2F(r), \quad (98)$$

where  $F$  is defined by (87). Recall that  $F$  has a zero at  $r_0 \approx 0.6$  and a minimum at  $r_1 \approx 1$  and rapidly approaches 0 at large  $r$ . When  $s \gg u^{1/3}$ ,  $F_{P''}$  exceeds all nonlinear forces, in particular the PH force (which, we have seen, dominates the nonlinear forces if  $s \ll u$ ). Whether the total force is attractive or repulsive at large  $s$  is determined by the relative size of the two constant forces in (98), and hence on the value of  $r$ ,  $F(u)$  being small and negative. (1) For  $r_0 < r \ll u$  and  $r$  not too close to  $r_0$ ,  $F_{P''}$  dominates and the total force is attractive. This is the regime in which the cutoff model seems most trustworthy physically. In particular, it contains the point  $r_1$ , which one might regard as the most “natural” value, corresponding to two blocks of material in relaxed contact, their effective surfaces separated by the typical interatomic spacing. (2) For

$0 \leq r < r_0$  and  $r$  not too close to  $r_0$ ,  $F_{P''}$  again dominates and the total force is repulsive. In particular, if  $r = 0$  the two gap forces ( $P''$  and  $VP'$ ) cancel and the force can be attributed to the negative surface energy in the region  $\alpha$  (Fig. 5) and the similar region next to the part of the bullet outside the barrel. (3) If  $r = r_0$ ,  $F_{P''}$  vanishes and the long-range force is purely  $F_{PV}$ , the repulsive Lukosz force. This result is what the piston model was designed to achieve — a gedankenexperiment showing that the Lukosz result has, at least in principle, some physical reality. Unfortunately, that result is attainable only by fine-tuning and, moreover, by pushing  $r$  into a regime where the physical relevance of the cutoff model is questionable. (4) For a special value close to  $r_0$ , namely

$$r \approx r_0 + \frac{F(u)}{2F'(r_0)} = r_0 - \frac{\zeta(3)}{32u^2F'(r_0)}, \quad (99)$$

the long-range linear force vanishes. In this scenario the force is the sum of the PH, PD, and VD terms; in the small-cutoff regime of interest, it is approximately the piston force (82). This force is always attractive, but exponentially weak at large  $s$ .

In short, the gap plays a spoiler role somewhat like that of the outer shaft in the piston model. In the piston, where shaft and chamber have the same width, the shaft force precisely cancels the related repulsive force from the VP paths in the chamber, leaving the Casimir-like force (82). The same occurs for the pistol in scenario 4, but in the more plausible scenario, 1, the (attractive,  $a$ -independent) gap force overwhelms the interior VP force, precisely because the gap is narrower than the chamber. In any case, the force arising from outside the chamber depends, not surprisingly, on the geometrical configuration outside the chamber, while the force arising inside is fixed by the geometry of the chamber.

For the reason mentioned in connection with parallel plates, the fact that the gap force becomes repulsive at all at finite gap size may be an artifact of the cutoff model. What one can say is that the even cruder model of perfect reflection also displays an artifact, in the form of an attractive force that diverges as the gap size approaches zero. In a more realistic model taking into account the interactions related to condensed matter physics one would expect the gap force to be reduced, if never reversed.

## 7 Conclusions

We have presented a thorough analysis of the vacuum expectation value of the stress-energy-momentum tensor in a rectangle. The calculational methods



involve an exponential ultraviolet cutoff and a sum over images (or closed reflecting paths). Here we have treated a two-dimensional scalar field; the extension to three dimensions and electromagnetism is straightforward and under way. Formulas are presented for all tensor components,  $T_{\mu\nu}(\mathbf{r})$ , for arbitrary combinations of Dirichlet and Neumann boundaries, arbitrary values of the curvature coupling  $\xi$ , and arbitrary values of the cutoff parameter, including the limit where the cutoff is removed. Forces (which are independent of  $\xi$ ) have been consistently calculated both by differentiating energy and by integrating pressure.

Studying the local energy density and stresses (rather than just total energy), using a physically motivated ultraviolet cutoff (rather than an “analytic” regularization scheme), and studying separately the contributions from various classes of specularly reflecting paths all help to interpret the physics, especially the roles of boundaries and corners. Within a cutoff framework one has a clear and consistent definition of energy densities and forces. When different configurations of rigid bodies are compared and all contributions (from inside and outside) are included, one always finds a cancellation of the energy divergences and hence an unambiguous force in the limit of no cutoff. The decomposition by paths helps one to understand better the cancellations of divergent terms and often to understand intuitively the sign of the Casimir force. Most strikingly, the force on one side of the rectangle includes important repulsive components associated with paths *parallel* to that side: a divergent term from short paths that reflect from the perpendicular sides, and a finite, constant term from periodic paths between the two perpendicular sides. In piston geometries these forces are cancelled by counterpart terms from the exterior of the rectangle, but in more general circumstances the problem of their physical interpretation must be taken seriously.

In the later sections of the paper we discuss geometries in which the vacuum forces from inside a rectangle might be rigorously exhibited. The box with a loose lid (Fig. 7) is closest to what one wants to understand, but accurate calculation of the external edge and, especially, corner effects remains impractical for now (at least, beyond the scope of the present paper). The piston model (Fig. 6) studied by previous authors is rigorous and exact, but it obscures the point at issue by adding an external shaft. Our attempt to compromise these two scenarios is the *pistol* (Fig. 8), which unfortunately did not yield a robust result. The force on the pistol depends sensitively on the cutoff length, as compared to the width of the gap between the bullet and the barrel. The only regime in which our quantitative analysis (extrapolated to 3D electromagnetism) can be regarded as physically trustworthy is that where the gap is small but still larger than the cutoff; there the behavior is cutoff-independent but the force is attractive. Scenarios where the net force is repulsive (in particular, one where the gap force vanishes) do exist, but require entering the regime where the calculations cannot be taken seriously on

a quantitative level because one does not know what the correct ultraviolet cutoff behavior is (and because stiction and friction are likely to be the dominant effects there); furthermore, making the gap force zero or small requires fine tuning within this regime. Nevertheless, although no quantitative claims can be made for our model (piston + cutoff) in that regime, we do submit that the model is closer to the physical truth than either a model without cutoff (which would predict infinite energies) or an analytic regularization that hides the divergences from the beginning. Furthermore, while the repulsive Lukosz component of the force is robust, the force opposing it is dependent on the scenario considered (e.g., piston vs. pistol, or wide gap vs. narrow) and could in principle be controlled to demonstrate the reality of the Lukosz force, even if the *net* force is attractive in all practical experiments.

## Acknowledgements

We thank Martin Schaden and Carlos Villarreal for discussions and for providing manuscript copies of their unpublished works. We thank Gabriel Barton for correspondence and Jef Wagner, Prachi Parashar, Chris Pope, and Wayne Saslow for useful remarks. The numerical plots in Sec. 6 were created with *Mathematica*, the other graphics with  $\text{\LaTeX}$ .

This research is supported by the linked NSF Grants PHY-0554849 (TAMU) and PHY-0554926 (OU) and forms part of our continuing collaboration with Ricardo Estrada. K. A. Milton also received support from DOE Grant DE-FG02-04ER41305. L. Kaplan is supported by NSF Grant PHY-0545390. K. Kirsten is supported by NSF Grant PHY-0757791.

## References

- [1] W. Lukosz, *Physica* 56 (1971) 109.
- [2] J. Ambjørn, S. Wolfram, *Ann. Phys.* 147 (1983) 1.
- [3] A. Actor, *Ann. Phys.* 230 (1994) 303.
- [4] J. S. Dowker, G. Kennedy, *J. Phys. A* 11 (1978) 895.
- [5] J. S. Dowker, R. Banach, *J. Phys. A* 11 (1978) 2255.
- [6] E. Elizalde, *Ten Physical Applications of Spectral Zeta Functions*, Springer, Berlin, 1995.
- [7] E. Elizalde, S. D. Odintsov, A. Romeo, A. A. Bytsenko, S. Zerbini, *Zeta Regularization Techniques with Applications*, World Scientific, Singapore, 1994.

- [8] K. Kirsten, *Spectral Functions in Mathematics and Physics*, Chapman & Hall/CRC, Boca Raton, 2002.
- [9] J. R. Ruggiero, A. Villani, A. H. Zimerman, *J. Phys. A* 13 (1980) 761.
- [10] L. S. Brown, G. J. Maclay, *Phys. Rev.* 184 (1969) 1272.
- [11] R. Balian, B. Duplantier, *Ann. Phys.* 104 (1977) 300 and 112 (1978) 165.
- [12] M. T. Jaekel, S. Reynaud, *J. Physique I* 1 (1991) 1395, and related papers by Reynaud et al.
- [13] M. Schaden, L. Spruch, *Phys. Rev. A* 58 (1998) 935.
- [14] F. D. Mazzitelli, M. J. Sánchez, N. N. Scoccola, J. von Stecher, *Phys. Rev. A* 67 (2003) 013807.
- [15] S. A. Fulling, in *Quantum Field Theory under the Influence of External Conditions* (proceedings of QFExt-6, Norman, OK, 2003), K. A. Milton, ed., Rinton Press, Princeton, 2004, pp. 166–174.
- [16] R. L. Jaffe, A. Scardicchio, *Phys. Rev. Lett.* 92 (2004) 070402.
- [17] A. Scardicchio, R. L. Jaffe, *Nucl. Phys. B* 704 (2005) 552 and 743 (2006) 249.
- [18] R. Balian, C. Bloch, *Ann. Phys.* 69 (1972) 76.
- [19] S. Hacyan, R. Jáuregui, C. Villarreal, *Phys. Rev. A* 47 (1993) 4204.
- [20] R. B. Rodrigues, N. F. Svaiter, *Physica A* 342 (2004) 529.
- [21] L. H. Ford, N. F. Svaiter, *Phys. Rev. D* 58 (1998) 065007.
- [22] N. Graham, K. D. Olum, *Phys. Rev. D* 67 (2003), 085014, and related papers by Graham et al.
- [23] S. A. Fulling, *J. Phys. A* 36 (2003) 6857.
- [24] K. A. Milton, *J. Phys. A* 37 (2004) 6391.
- [25] I. Cervero-Peláez, K. A. Milton, J. Wagner, *Phys. Rev. D* 73 (2006) 085004.
- [26] I. Cervero-Peláez, K. A. Milton, K. Kirsten, *J. Phys. A* 40 (2007) 3607.
- [27] R. M. Cavalcanti, *Phys. Rev. D* 69 (2004) 065015.
- [28] N. F. Svaiter, B. F. Svaiter, *J. Phys. A* 25 (1992) 979.
- [29] M. P. Hertzberg, R. L. Jaffe, M. Kardar, A. Scardicchio, *Phys. Rev. Lett.* 95 (2005) 250402.
- [30] M. P. Hertzberg, R. L. Jaffe, M. Kardar, A. Scardicchio, *Phys. Rev. D* 76 (2007) 045016.
- [31] A. Rodriguez, M. Ibanescu, D. Iannuzzi, F. Capasso, J. D. Joannopoulos, S. G. Johnson, *Phys. Rev. Lett.* 99 (2007) 080401.

- [32] A. Rodriguez, M. Ibanescu, D. Iannuzzi, J. D. Joannopoulos, S. G. Johnson, Phys. Rev. A 76 (2007) 032106.
- [33] S. Zaheer, A. W. Rodriguez, S. G. Johnson, R. L. Jaffe, Phys. Rev. A 76 (2007) 063816.
- [34] W. Lukosz, Z. Physik 262 (1973) 327.
- [35] D. Deutsch, P. Candelas, Phys. Rev. D 20 (1979) 3063.
- [36] J. S. Dowker, Phys. Rev. D 36 (1987) 3095, and related papers.
- [37] A. G. Smith, in The Formation and Evolution of Cosmic Strings, G. Gibbons, S. Hawking, and T. Vachaspati, eds., Cambridge U. P., Cambridge, 1990, pp. 263–292.
- [38] M. E. X. Guimarães and B. Linet, Commun. Math. Phys. 165 (1994) 297.
- [39] K. A. Milton, P. Parashar, J. Wagner, Phys. Rev. Lett. 101 (2008) 160402.
- [40] K. A. Milton, P. Parashar, J. Wagner, to appear in volume in honor of I. Brevik (S. D. Odintsov, ed.), TSPU Vestnik (arXiv:0811.0128); J. Wagner, K. A. Milton, P. Parashar, to appear in proceedings of 60 Years of the Casimir Effect, Brasilia, June 2008 (arXiv:0811.2442).
- [41] Z. H. Liu, Ph.D. dissertation, Texas A&M University, in preparation.
- [42] R. Estrada, S. A. Fulling, L. Kaplan, K. Kirsten, Z. Liu, K. A. Milton, J. Phys. A 41 (2008) 164055.
- [43] S. L. Lebedev, Zh. Eksp. Teor. Fiz. 110 (1996) 769 [JETP 83, 423].
- [44] A. A. Saharian, Phys. Rev. D 69 (2004) 085005.
- [45] S. A. Fulling, Aspects of Quantum Field Theory in Curved Space-Time, Cambridge U. P., Cambridge, 1989.
- [46] Z. H. Liu, S. A. Fulling, New J. Phys. 8 (2006) 234.
- [47] M. Kac, Amer. Math. Monthly 73 Part II (1966) 1.
- [48] C. Clark, SIAM Rev. 9 (1967) 627.
- [49] P. B. Gilkey, Invariance Theory, the Heat Equation and the Atiyah–Singer Index Theorem, CRC Press, Boca Raton, 1995.
- [50] S. A. Fulling, Bull. Amer. Mat. Soc. 43 (2006) 423.
- [51] F. Bernasconi, G. M. Graf, D. Hasler, Ann. Henri Poincaré 4 (2003) 1001.
- [52] T. H. Boyer, Phys. Rev. 174 (1968) 1764.
- [53] G. Barton, Phys. Rev. D 73 (2006) 065018.
- [54] V. N. Marachevsky, Phys. Rev. D 75 (2007) 085019.

- [55] A. Edery, Phys. Rev. D 75 (2007) 105012.
- [56] X.-H. Zhai, X.-Z. Li, Phys. Rev. D 76 (2007) 047704.
- [57] M. Schaden, L. Mateescu, talk at American Physical Society meeting, March 2007 (arXiv:0705.3435).
- [58] V. N. Marachevsky, J. Phys. A 41 (2008) 164007.
- [59] A. Edery, I. MacDonald, J. High Energy Phys. 09 (2007) 005.
- [60] A. Edery, V. Marachevsky, Phys. Rev. D 78 (2008) 025021.
- [61] H. Cheng, Phys. Lett. B 668 (2008) 72.
- [62] M. Schaden, Phys. Rev. Lett., in press (arXiv:0808.3966).
- [63] H. Gies, K. Klingmüller, J. Phys. A 39 (2006) 6415.
- [64] A. W. Rodriguez, J. D. Joannopoulos, S. G. Johnson, Phys. Rev. A 77 (2008) 062107.
- [65] G. Barton, J. Phys. A 34 (2001) 4083.
- [66] V. N. Marachevsky, Physica Scripta 64 (2001) 205.
- [67] I. Brevik, G. Einevoll, Phys. Rev. D 37 (1988) 2977.
- [68] K. A. Milton, Y. J. Ng, Phys. Rev. E 55 (1997) 4207.
- [69] K. A. Milton, unpublished.
- [70] G. Barton, J. Phys. A 37 (2004) 1011.
- [71] G. Barton, J. Phys. A 38 (2005) 2997 and 3021.
- [72] G. J. Maclay, C. Villarreal, A model for Casimir forces in closed cavities with finite conductivity, unpublished (2003).
- [73] G. Mahajan, T. Padmanabhan, S. Sarkar, Phys. Lett. B 641 (2006) 6.
- [74] L. Perivolaropoulos, Phys. Rev. D 77 (2008) 107301.
- [75] M. Abramowitz, I. A. Stegun, eds., Handbook of Mathematical Functions with Formulas, Graphs, and Mathematical Tables (National Bureau of Standards Applied Mathematics Series, No. 55), 7th printing, U.S. Government Printing Office, Washington, 1968.
- [76] O. Kenneth, I. Klich, Phys. Rev. Lett. 97 (2006) 160401.
- [77] C. P. Bachas, J. Phys. A 40 (2007) 9089.